University of Illinois at Urbana-Champaign

ACRC

Air Conditioning and Refrigeration Center A National Science Foundation/University Cooperative Research Center

Investigation of an R134A Refrigerant/Iso 32 Polyol Ester Oil Mixture in Condensation

W. T. Piggott, III, T. A. Newell, and J. C. Chato

ACRC TR-192 December 2001

For additional information:

Air Conditioning and Refrigeration Center
University of Illinois
Mechanical & Industrial Engineering Dept.
1206 West Green Street
Urbana, IL 61801

(217) 333-3115

Prepared as part of ACRC Project #120
Investigation of Refrigerant/Oil Mixtures in Horizontal Tubes and Flat Plate Condensers and Evaporators
T. A. Newell and J. C. Chato, Principal Investigators

The Air Conditioning and Refrigeration Center was founded in 1988 with a grant from the estate of Richard W. Kritzer, the founder of Peerless of America Inc. A State of Illinois Technology Challenge Grant helped build the laboratory facilities. The ACRC receives continuing support from the Richard W. Kritzer Endowment and the National Science Foundation. The following organizations have also become sponsors of the Center.

Alcan Aluminum Corporation
Amana Refrigeration, Inc.
Arçelik A. S.
Brazeway, Inc.
Carrier Corporation
Copeland Corporation
Dacor
Daikin Industries, Ltd.
Delphi Harrison Thermal Systems
General Motors Corporation
Hill PHOENIX
Honeywell, Inc.
Hydro Aluminum Adrian, Inc.
Ingersoll-Rand Company
Invensys Climate Controls
Kelon Electrical Holdings Co., Ltd.
Lennox International, Inc.
LG Electronics, Inc.
Modine Manufacturing Co.
Parker Hannifin Corporation
Peerless of America, Inc.
Samsung Electronics Co., Ltd.
Tecumseh Products Company
The Trane Company
Valeo, Inc.
Visteon Automotive Systems
Wolverine Tube, Inc.
York International, Inc.

For additional information:

Air Conditioning & Refrigeration Center
Mechanical & Industrial Engineering Dept.
University of Illinois
1206 West Green Street
Urbana, IL 61801

217 333 3115

Table of Contents

List of Figures

Page

List of Tables

Page

Nomenclature

A	Area (m2)	
cp	Specific Heat	
D	Diameter	
Ft	Froude rate	$= \left[\frac{x^3 G^2}{\rho_v{}^2 g D (1-x)} \right]^{\frac{1}{2}}$
G	Mass Flux (kg/m2s)	
k	Thermal Conductivity	
K	Smith's entrainment ratio	
KH	Hughmark correction factor	
L	Tube Length (m)	
m	Mass (kg)	
mo	Predicted Maximum Oil	Equation 5.1
mox	Predicted Oil Holdup	Equation 5.2
mr	Refrigerant Mass	
mf	Full Test Section Mass	
me	Evacuated Test Section Mass	
mt	Towel Mass	
moil	Mass of Oil in Test Section	
$\dot{m}$	Mass Flow Rate (kg/s)	
P.I.	Property Indices	Equations 2.1, 2.2
Re	Reynolds Number	$= \frac{GD_i}{\mu}$
Rel	Liquid Reynolds number	$= \frac{GD_i(1-x)}{\mu_l}$
Rev	Vapor Reynolds Number	$= \frac{GxD_i}{\mu_v}$
S	Slip ratio	Equation 2.6
T	Temperature (°C)	
Tsat	Saturation Temperature (°C)	
v	Specific Volume	
Vl	Liquid Velocity	
Vv	Vapor Velocity	
Vts	Test Section Volume	
Vtemp	Temporary Test Section Volume	Equation 3.5
Voil	Oil Volume	
x	Quality	
xr	Refrigerant Mass Fraction	$\left(\frac{\text{refrigeran t mass}}{\text{total liquid mass}} \right)$

x_o	Oil Mass Fraction	$\left(\frac{\text{oil mass}}{\text{total liquid mass}}\right)$
x_s	Static quality	
X_{tt}	Lockhart-Martinelli parameter	Equation 2.11
X_{vt}	Lockhart-Martinelli parameter	Equation 2.12
X_{tv}	Lockhart-Martinelli parameter	Equation 2.13
X_{vv}	Lockhart-Martinelli parameter	Equation 2.14
a	Void Fraction	
μ	Viscosity	
μ_f	Viscosity of liquid	
μ_l	Viscosity of saturated liquid	
μ_g	Viscosity of saturated vapor (gas)	
ρ	Density	
ρ_l	Density of saturated liquid	
ρ_g	Density of saturated vapor (gas)	

Common Subscripts

f	Liquid/ fluid
g	Vapor/ gas
l	Liquid
lo	Liquid Only
m	Mixture
m_1	Mixture Component
m_2	Mixture Component
v	Vapor

Chapter 1: Introduction

Two-phase flow in air-conditioning and refrigeration vapor compression systems generally consists of a mixture of refrigerant and lubricating oil. Void fraction is an important property within these flows, as it can be used to determine required system refrigerant charge. Also, as the lubricating oil level to keep the compressor functioning is dependent on the amount of oil circulating through a system. This study investigates void fraction and oil hold-up for refrigerant-oil mixtures to help reach an understanding of the effects and behavior of refrigerant/oil mixtures in systems.

This study consisted of the study of R134a refrigerant and polyol ester oils in horizontal copper tubes. Three types of round copper tube were used, each with a 9.52 mm (3/8") outer diameter, and 8.91 mm (0.351") inner base diameter. One tube used was internally smooth, while the other two were microfinned tubes, with 0° (axially grooved) and 18° helix angle. Tests were conducted at two flowing oil concentration ranges: 0.2-0.4% and 3-5% oil by mass concentration.

This document is made up of 6 chapters. Chapter 2 reviews literature on void fraction. Experimental facilities and procedures will be discussed in Chapter 3. Chapter 4 will present the void fraction and oil hold-up data, while Chapter 5 will hold the analysis of that data. Chapter 6 will be a concluding chapter.

Chapter 2: Literature Review

This literature review will address void fraction models in literature, as well as the effects of oil when mixed with refrigerant. The parameters used in the various void fraction models will be discussed here as well.

2.1 Void Fraction Review

Void fraction (a) literature has been reviewed in a series of Air-Conditioning and Refrigeration Center (ACRC) technical papers, including Wilson et al. (2001), Tran et al. (2000), Gupta et al. (2000), Graham et al. (1998a), Kopke et al. (1998), Wilson et al.(1998), and Yashar et al. (1998). Rice (1987), was referenced in all the previously mentioned reports, and presented a review of a variety of void fraction models found in various publications. This paper by Rice differentiated the existing models into four types: homogenous, slip-ratio, Lockhart-Martinelli, and mass-flux dependent. These divisions were based on the main effects used to model void fraction. Rice also defined two property ratio indices for two-phase flow, which are listed here.

$$P.I._1 = \frac{\rho_v}{\rho_l} \tag{2.1}$$

$$P.I._2 = \left(\frac{\mu_l}{\mu_v}\right)^{0.2} \frac{\rho_v}{\rho_l} = \left(\frac{\mu_l}{\mu_v}\right)^{0.2} \cdot P.I._1 \tag{2.2}$$

2.1.1 Homogenous Model

The homogenous model for two phase flow is the model for both phases flowing as a single fluid with equal velocity. This model gives an effective upper bound for the void fraction data seen experimentally. Also included here are the property equations for homogenous flow, which give the flow properties as a void fraction weighted average of the single phase properties.

$$\alpha = \frac{1}{1+\left(\frac{1-x}{x}\right)\left(\frac{\rho_v}{\rho_l}\right)} \tag{2.3}$$

$$? = ?_v a + ?_l (1-a) \tag{2.4}$$

$$\mu = \mu_v a + \mu_l (1-a) \tag{2.5}$$

2.1.2 Slip-Ratio Models

Slip-ratio models are similar to the homogenous model, but include a term that takes into account the vapor and liquid phases in the flow moving at different speeds. This term is the slip ratio (S), which is calculated differently according to various correlations, and is the ratio of vapor to liquid velocity. Slip ratio and void fraction are generally defined as shown below.

$$S = \frac{V_v}{V_l} \tag{2.6}$$

$$a = \frac{1}{1+\left(\frac{1-x}{x}\right)\left(\frac{?_v}{?_l}\right)\bullet S} \tag{2.7}$$

As can be seen by examining the above equations, the homogenous model can be interpreted as a special case of the slip ratio model where S=1.

An analytical slip ratio model was devised by Zivi (1964), using the principle of minimum entropy production. Zivi assumed the flow was steady state, and annular (the liquid in an annulus along the tube wall). Also assumed were that wall friction was negligible, and no liquid was entrained in the vapor core of the flow. Zivi let the exiting void fraction determine the energy dissipation of the system, and then analyzed the flow to minimize entropy production. This model resulted in the expressions for slip ratio and void fraction shown below.

$$S = \left(\frac{\rho_l}{\rho_v}\right)^{\frac{1}{3}} \tag{2.8}$$

$$\alpha = \frac{1}{1+\left(\frac{1-x}{x}\right)\left(\frac{\rho_v}{\rho_l}\right)^{\frac{2}{3}}} \tag{2.9}$$

Smith (1969) derived a void fraction model based on the following assumptions: the flow is annular with a homogenous mixture phase and a pure liquid phase, the velocity heads of each phase are equal ($\rho_l V_l^2=\rho_m V_m^2$), the mixture phase acts as a single fluid with a variable density, and thermal equilibrium exists which allows a heat balance to determine the amount of vapor present. Smith's model was based on steam flow, and named a variable K as the ratio of the water mass flow in the mixture phase to the total water mass flow. From these assumptions, the slip ratio can be calculated as shown in equation 2.10.

$$S = K + (1-K)\left[\frac{\frac{\rho_l}{\rho_v} + K\left(\frac{1-x}{x}\right)}{1+K\left(\frac{1-x}{x}\right)}\right]^{\frac{1}{2}} \tag{2.10}$$

Smith found that a K value of 0.4 agreed with experimental steam and air-water data within approximately 10%.

2.1.3 Lockhart-Martinelli Models

The following set of void fraction models are based on the Lockhart-Martinelli parameter (1949). The parameter is defined for different combinations of turbulent (t), and laminar (v) flow. The appropriate form is taken based on the Reynolds number (Re) for each individual phase. The flow is considered laminar if Re <1000, and turbulent if Re > 2000. The liquid phase condition is noted first in the parameter subscripts, so for example X_{vt} indicates laminar liquid flow with turbulent vapor flow.

$$X_{tt} = \left(\frac{1-x}{x}\right)^{0.9}\left(\frac{\rho_v}{\rho_l}\right)^{0.5}\left(\frac{\mu_l}{\mu_v}\right)^{0.1} \tag{2.11}$$

$$X_{vt} = \left[\frac{C_f}{C_g}\frac{1}{Re_g^{0.8}}\left(\frac{1-x}{x}\right)\frac{?_g}{?_f}\frac{\mu_f}{\mu_g}\right]^{0.5} \tag{2.12}$$

$$X_{tv} = \left[\frac{C_f}{C_g}Re_f^{0.8}\left(\frac{1-x}{x}\right)\frac{?_g}{?_f}\frac{\mu_f}{\mu_g}\right]^{0.5} \tag{2.13}$$

$$X_{vv} = \left(\frac{1-x}{x}\right)^{0.5}\left(\frac{?_v}{?_l}\right)^{0.5}\left(\frac{\mu_l}{\mu_v}\right)^{0.5} \tag{2.14}$$

The two-phase Reynolds number used in the above equations is defined as shown here.

$$Re_g = \frac{xGD}{\mu_g} \tag{2.15}$$

$$Re_f = \frac{(1-x)GD}{\mu_f} \tag{2.16}$$

Baroczy (1965) developed a model using liquid mercury-nitrogen and air-water experimental data. This model was in the tabular form, being determined by X_{tt} and P.I.$_2$, and specified liquid fraction $(1-a)$. The table used for this model is presented here.

Table 2-1: Baroczy Correlation

	X_{tt}										
P.I.2	0.01	0.04	0.1	0.2	0.5	1	3	5	10	30	100
	Liquid Fraction (1-α)										
0.00002				0.0012	0.009	0.068	0.17	0.22	0.30	0.47	0.71
0.0001			0.0015	0.0054	0.030	0.104	0.23	0.29	0.38	0.57	0.79
0.0004		0.0022	0.0072	0.180	0.066	0.142	0.28	0.35	0.45	0.67	0.85
0.001	0.0018	0.0066	0.0170	0.0345	0.091	0.170	0.32	0.40	0.50	0.72	0.88
0.004	0.0043	0.0165	0.0370	0.0650	0.134	0.222	0.39	0.48	0.58	0.80	0.92
0.01	0.0050	0.0210	0.0475	0.0840	0.165	0.262	0.44	0.53	0.63	0.84	0.94
0.04	0.0056	0.0250	0.0590	0.1050	0.215	0.330	0.53	0.63	0.72	0.90	0.96
0.1	0.0058	0.0268	0.0640	0.1170	0.242	0.380	0.60	0.70	0.78	0.92	0.98
1	0.0060	0.0280	0.0720	0.1400	0.320	.500	0.75	0.85	0.90	0.94	0.99

Wallis (1969) fit a correlation to Lockhart and Martinelli's void fraction data that was presented with their two-phase pressure drop data. Wallis stated that as the frictional portion of the pressure drop decreased with respect to other terms, the error of this correlation increased.

$$\alpha = \left(1 + X_{tt}^{0.8}\right)^{-0.378} \tag{2.17}$$

Domanski et al. (1983) modified the Wallis correlation to fit a wider range of conditions as defined by the X_{tt} parameter. The equations below show the adjusted model, as well as the X_{tt} ranges for the two forms.

$$\alpha = \left(1 + X_{tt}^{0.8}\right)^{-0.378} \qquad X_{tt}<10 \tag{2.18}$$

$$\alpha = .823 - .157 \cdot \ln\left(X_{tt}\right) \qquad 10<X_{tt}<189 \tag{2.19}$$

2.1.4 Mass Flux Dependent Models

Graham et al. (1998a) produced a model based on experimental work involving R134a and R410A condensing in a horizontal tube at the ACRC. This correlation includes the Froude Rate parameter (Ft) derived by Hurlburt and Newell (1997), and defined below with Graham's model.

$$Ft = \left[\frac{x^3 G^2}{\rho_v^2 g D(1-x)}\right]^{\frac{1}{2}} \tag{2.20}$$

$$\alpha = 1 - \exp\left[-1 - 0.3 \cdot \ln(Ft) - 0.0328 \cdot (\ln(Ft))^2)\right] \qquad Ft>0.01032 \tag{2.21}$$

$$\alpha = 0 \qquad Ft<0.01032 \tag{2.22}$$

Graham et al.(1998b) further modified the Wallis correlation to include mass flux effects seen in the experimental data. This model is suggested for use in refrigerant condensation and evaporation in smooth tubes.

$$\alpha = (1 + X_{tt} + 1/Ft)^{-0.321} \tag{2.23}$$

Yashar et al. (2000) suggested using the above model for smooth tubes and microfin tubes in evaporation conditions, but recommended the slightly different form following for microfin tubes in condensation. The combination of these two models will be referred to as the ACRC void fraction model for the rest of this text.

$$\alpha = (1 + X_{tt} + 1/Ft)^{-0.375} \tag{2.24}$$

2.2 Refrigerant/ Oil Mixture Review

The effects of oil when mixed with refrigerant have been studied widely, as this is the type of working fluid present in most working vapor compression refrigeration systems. One of the issues that arises when these mixtures are in use is the determination of fluid properties, which are addressed in some of the following references. Gaibel et al. (1994) reviews some of the issues involved with refrigerant/oil mixtures in general, and properties in particular. Two methods used to account for oil addition to refrigerants are to use mixture correlations for the thermodynamic properties, as seen in Baustian et al. (1986). Another method, used by Tichy et al. (1985), is to use pure refrigerant property models and then apply a correction factor.

Reid et al. (1987) listed several methods for calculating mixture properties, among them the linear method, which is shown here for density, viscosity, specific heat, and thermal conductivity.

$$? = x_{m_1} ?_{m_1} + (1 - x_{m_1}) ?_{m_2} \tag{2.25}$$

$$\mu = x_{m_1}\mu_{m_1} + (1 - x_{m_1})\mu_{m_2} \tag{2.26}$$

$$c_P = x_{m_1}c_{Pm_1} + (1 - x_{m_1})c_{Pm_2} \tag{2.27}$$

$$k = x_{m_1}k_{m_1} + (1 - x_{m_1})k_{m_2} \tag{2.28}$$

The linear model assumes ideal mixing of the refrigerant and oil. However, particularly for miscible oils the effect of mixing the two fluids is non-ideal. Indeed, the viscosity of the liquid phase, where the oil is mainly present due to its very low vapor pressure, exhibits very non-ideal mixing behavior.

Baustian et al. (1986) used the following equation to take into account these non-ideal effects when mixing refrigerant with oil.

$$\mu_m = \left(x_r\mu_r^{1/3} + x_o\mu_o^{1/3}\right)^3 \tag{2.29}$$

Cawte et al. (1996) used the following equation to determine viscosity for their study of R12 and R22 in evaporation when mixed with lubricating oil.

$$\mu_m = \mu_r \exp\left(x_r\left[\frac{\mu_o}{\mu_r}\right]^{0.3}\right) \tag{2.30}$$

It should be noted that these models are used to determine the liquid properties, as the low vapor pressure of the oil results in the vapor phase being pure refrigerant. Figures 2.1 and 2.2 show a comparison of the models for the oil concentrations tested.

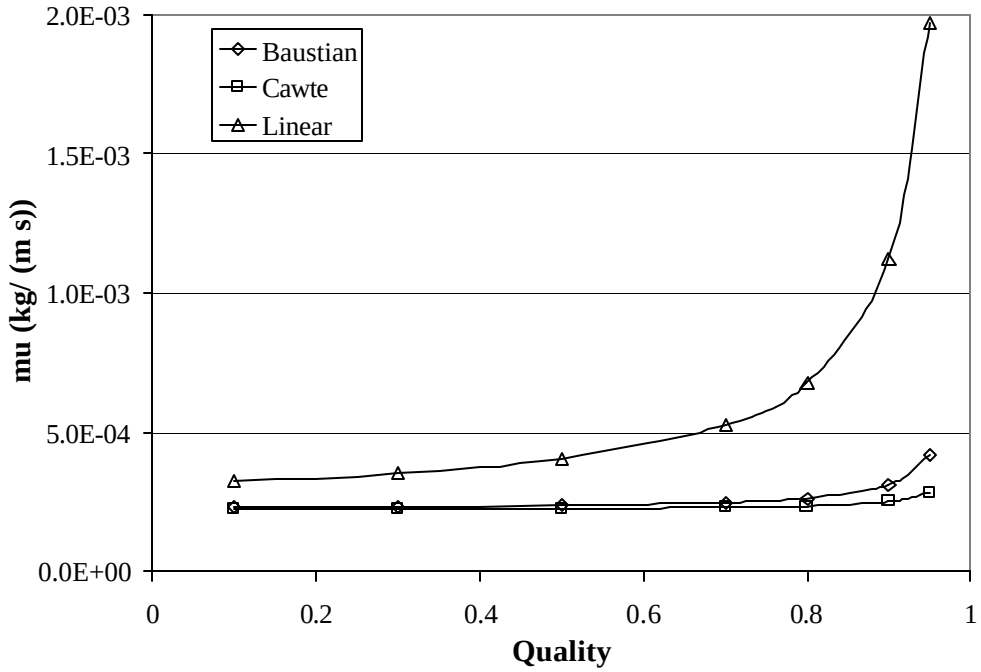

Figure 2.1: Viscosity vs. Quality for 0.3% ISO 32 POE/ R134a mixture, separated by mixture model

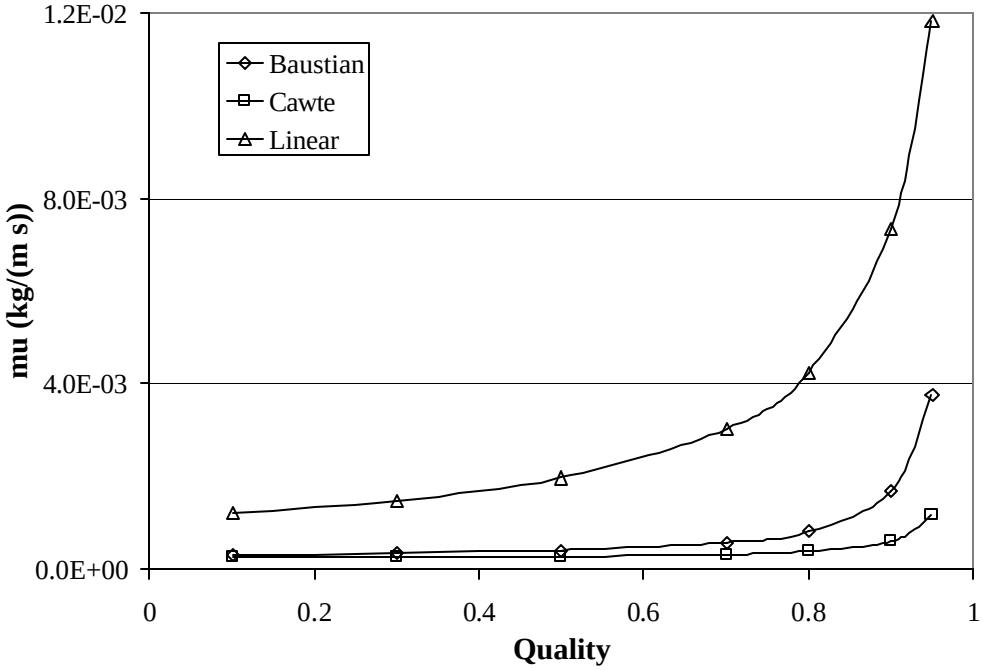

Figure 2.2: Viscosity vs. Quality for 3% ISO 32 POE/ R134a mixture, separated by mixture model

Chapter 3: Experimental Facility and Procedure

An existing two-phase refrigerant loop in the Air-Conditioning and Refrigeration Center at the University of Illinois at Urbana-Champaign was used for this study. Detailed descriptions of this apparatus can be found in Dobson (1994), Graham (1997), Kopke (1998), and Wilson (2001). This chapter will present a brief outline of this facility and describe the measurement techniques used to determine void fraction and oil hold-up for this study.

3.1 Refrigerant Loop

Figure 3.1 is a schematic of the experimental loop used. A receiver tank serves to separate liquid and vapor refrigerant. The receiver tank sits in a water bath whose temperature can be regulated by adding ice or use of electric heaters. Liquid refrigerant is drawn from the receiver tank through a shell and tube heat exchanger using cold building water to ensure subcooled liquid exiting the exchanger. The subcooled liquid is then drawn through a magnetically coupled pump that moves the refrigerant through the loop. Use of a pump instead of a compressor does not require the introduction of lubricating oil into the loop. Thus, oil can be added as needed for the experiments only, and be controlled or left out as necessary. After the pump the refrigerant passes through a Micro-Motion® Coriolis type mass flow meter. Next, the refrigerant flow enters a preheater section. For the first set of tests run with ISO32 POE oil this section consisted of three passes of tube wrapped with electric resistance heater strips. A drawback of this section was that it made it difficult to reach high qualities, as wall dryout in the tube caused failure (burn-out) of the electric strip heaters. A new preheater section was created and added to the loop. This section consisted of seven passes of 9.53 mm outer diameter copper tube. This tube section was sandwiched between two 6.35 mm thick aluminum plates (1.15 m x 0.36 m), and then flattened to a height of 6.35 mm. This was done based on results obtained by Wilson (2001) which showed that a slight amount of tube flattening provided enhanced heat transfer with an acceptable amount of added pressure drop. Attached to the outside of these plates are four Vulcan Electric strip heaters, each rated at 1500 W. However, the actual power supply in the room gives each heater an output of approximately 1 kW, with the total preheater having about 4 kW of heat addition capability. The use of the aluminum plates enables heat to conduct throughout the tube section to enter the refrigerant, and preventing overheating and failure of the heaters themselves. This new preheater section enables the loop to reach much higher quality levels, including the superheated vapor region. After the preheater, the refrigerant flow enters the test section. After the test section, the flow enters a water-cooled flat plate heat exchanger for removal of the heat added in by the preheaters. Following this heat exchanger, the refrigerant flows back into the receiver tank, forming a continuous loop. The pump and its bypass valve control the loop mass flow, with quality being set by the preheater, and the temperature of the receiver tank bath controlling the loop saturation temperature.

3.2 Test Section

The test sections used for this study consisted of three types of round copper single-pass tubes. Internally, one tube has a smooth cross-section, while the two enhanced tubes had fins placed at a 0° helix angle (axial) or an 18° helix angle. All three tubes had an outside diameter of 9.53 mm (3/8”). The tube wall thickness was 0.3 mm (0.012”), and the enhanced tubes had a fin height of 0.2 mm (0.008”). Each test section consisted of a 1.524 m (60”) section of tube with Hoke ball valves placed on each end. On the other end of each valve was a 9.53 mm o.d.

aluminum quick disconnect manufactured by Visteon. The valves and disconnects enable the section to be sealed off and removed from the refrigerant loop.

3.3 Test Conditions

Tests were conducted using R134a refrigerant at a 35° C inlet temperature. The oil used was an ICI RL32S polyol ester refrigeration oil. Two flowing oil concentration levels were tested: 0.2-0.4% and 3-5% oil by mass. These two ranges were used to simulate the level of oil circulating through operating systems. The low (0.2-0.4%) range simulates stationary compressors, where most of the lubricating oil stays in the compressor, possibly in a sump. The high (3-5%) range is used to model mobile (automotive) systems, where all the oil is in circulation through the system. The refrigerant mass fluxes tested were 75 and 150 kg/ (m^2 s), as allowed by the experimental apparatus. The flow qualities tested ranged from 10-70% for tests performed with the initial preheater section, and 10-95% for tests run with the new preheater section.

3.4 Experimental Procedure

The experimental procedure used consisted of several steps. First, before the test sections were used in the refrigerant loop, the volume in each test section had to be calculated. Then, the loop had to be set to the desired operating conditions, after which the void fraction and oil hold-up could be determined.

3.4.1 Test Section Volumes

The volumes of the test sections used were determined experimentally, using a method similar to that of Wilson (1998). Thermocouples were placed on the outside of the section, and a fitting was placed on a quick disconnect on one end of the section to enable charging and evacuation of the section. This fitting also had a pressure tap which lead to a pressure gauge, which was used to determine the pressure in the test section when charged with gas. The section was evacuated, and then charged with pure vapor for one of three gases: R134a, R22, and nitrogen. The pressure in the section was recorded, and the temperature was recorded as well. The fitting was removed, and the test section was then weighed. After this weight was recorded, the test section was evacuated and then weighed again. This procedure was repeated at least three times with each test gas used. Through this procedure the mass of gas in the section was obtained, as well as the temperature and pressure. Engineering Equation Solver (EES) was used with its gas property values to compute the average volume found by the tests conducted, which was then used as the test section volume for void fraction measurements, and designated V_{ts}.

3.4.2 Void Fraction and Oil Hold-Up Measurement

The technique for void fraction measurement used is similar to that of Gupta (2000), Wilson (2000,1998), and Sacks (1975). After the loop reaches the desired operating point, the two valves at each end of the test section are closed simultaneously, and a bypass line is opened. The test section is then removed from the refrigerant loop and weighed (m_f). Then a paper towel is weighed and attached to one end of the test section. The valve on this end of the section is then opened a small amount, allowing the refrigerant to slowly vent out. The purpose of this is to allow the refrigerant to be removed from the test section while leaving any oil in the section. After all the refrigerant has been vented from the test section, the towel is removed from the end and weighed (m_t). The towel is put in place to catch any oil that may be vented from the section due to the valve have been opened enough to vent out oil. The valve on the other end of the test section is then opened to remove any trapped refrigerant from within

the valve. Next, the test section is evacuated and weighed (m_e). Tests were run using wadding in the evacuation fittings that showed that oil was not removed from the section during this evacuation procedure. Following this, liquid refrigerant was washed through the test section to remove the oil held up in the test section. This was accomplished by connecting a recovery tank with clean refrigerant at room temperature to one end of the section, and attaching a recovery tank with refrigerant and oil mixed together in an ice bath to the other end of the section. The test section and hoses were then evacuated, after which three rinses using liquid refrigerant were run through the test section. Three rinses were used as this was determined to be the point at which further rinses do not significantly change the test section 'clean' weight (rinsed weight, without oil.) After rinsing, the test section is weighed for a final time (m_s). From these measurements the mass of refrigerant in the section is calculated using equation 3.1.

$$m_r = m_f - m_e \tag{3.1}$$

Next, the mass of oil in the test section is calculated, including any oil left on the paper towel during venting.

$$m_{oil} = m_e - m_s + m_t \tag{3.2}$$

The volume of the oil caught is then calculated using the density value provided by the manufacturer, as in equation 3.3. This volume is then subtracted from the test section volume to give a temporary refrigerant volume (V_{temp}).

$$V_{oil} = m_{oil} / ?_{oil} \tag{3.3}$$

$$V_{temp} = V_{ts} - V_{oil} \tag{3.4}$$

The specific volume of the refrigerant trapped in the test section is then calculated using equation 3.5. The static refrigerant quality is then calculated, using the inlet temperature to compute refrigerant property values. The static quality is then used to compute the void fraction for the refrigerant only in the test section, seen in equation 3.7. Then, the refrigerant vapor volume is determined and used to calculate the total void fraction, as shown in equations 3.8-3.9. The experimental void fraction values were then used as detailed in chapter 4 to determine void fraction using different analysis techniques.

$$v_{ref} = \frac{V_{temp}}{m_r} \tag{3.5}$$

$$x_{st} = \frac{v_{ref} - v_l}{v_v - v_l} \tag{3.6}$$

$$a_{ref} = \frac{1}{1 + \left(\frac{1 - x_{st}}{x_{st}}\right)\frac{?_v}{?_l}} \tag{3.7}$$

$$V_v = a_{ref} V_{temp} \tag{3.8}$$

$$a = V_v / V_{ts} \tag{3.9}$$

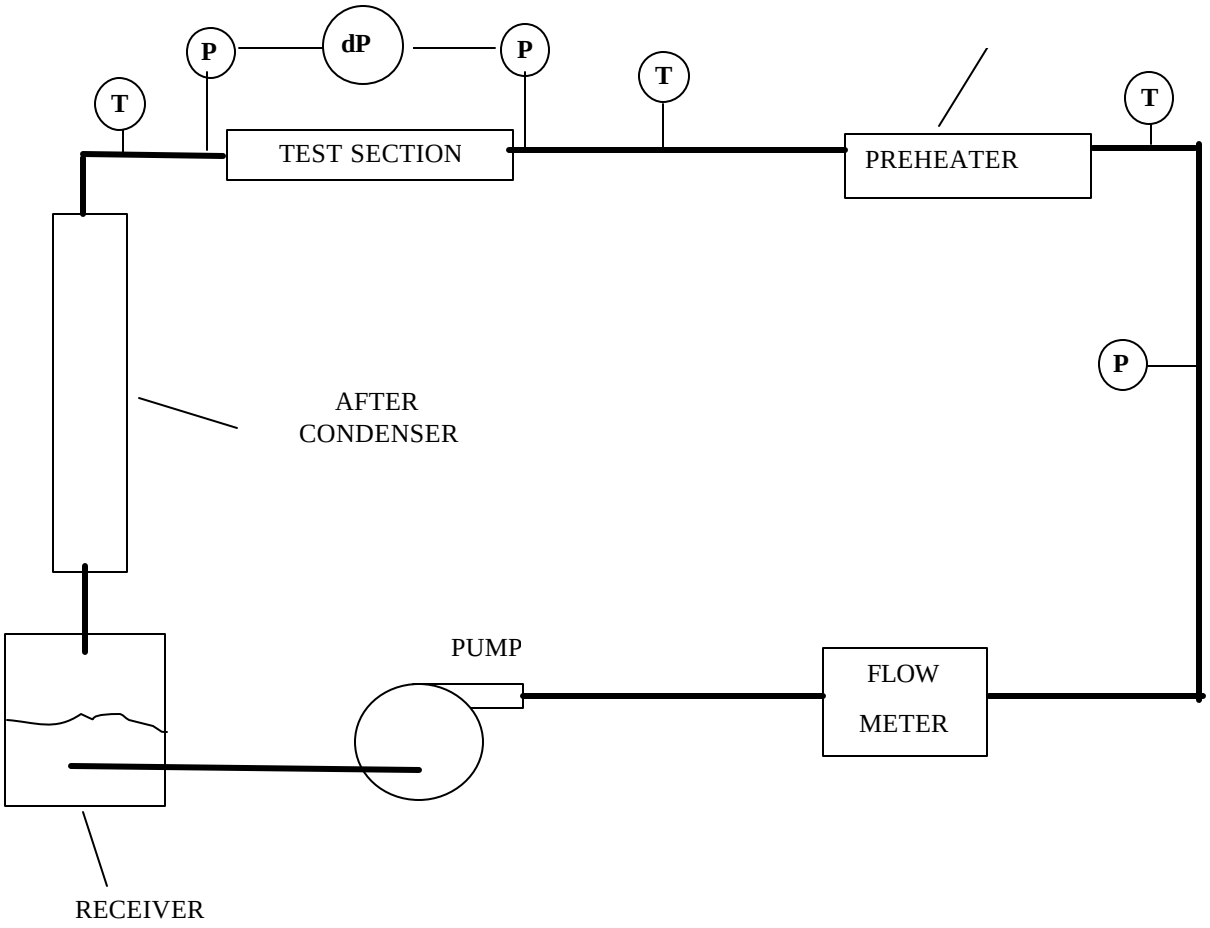

Figure 3.1: Schematic of experimental apparatus

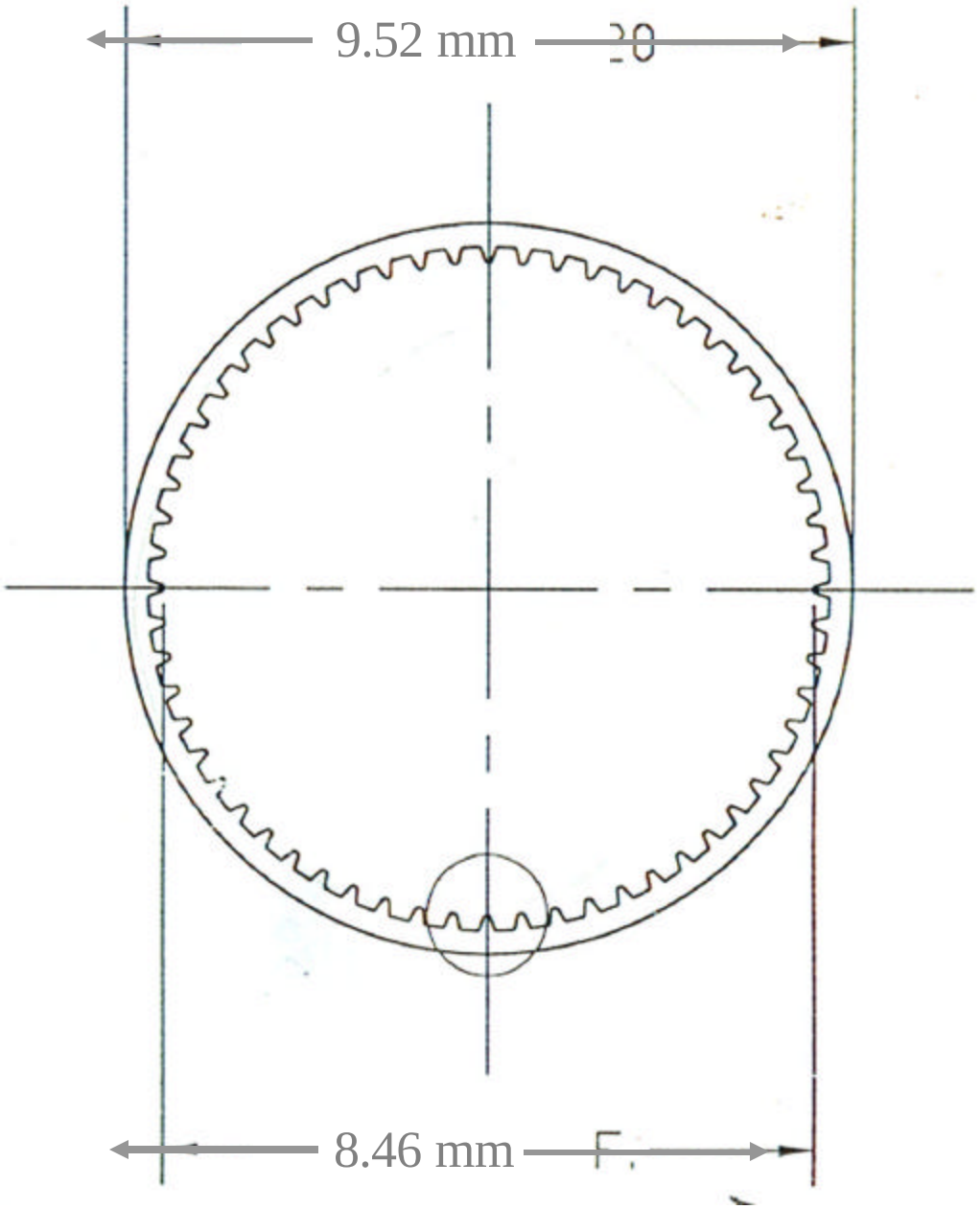

Figure 3.2: End View of Microfin Tube

Chapter 4: Experimental Results

This chapter will lay out the raw experimental results. The void fraction and oil holdup data is calculated as set forth in Chapter 3. The experimental results are shown graphically in the figures at the end of this chapter, and the raw data can be found in Appendix B.

4.1 Void Fraction Results

The void fraction results for this study can be grouped using several parameters including quality, mass flux, tube type, and oil concentration. The effects of these different conditions on the resulting void fraction will be analyzed. The uncertainty in the range of void fraction measurements ranged from 10% at low qualities to 5% at high qualities.

4.1.1 Effect of Quality on Void Fraction

The effect of quality on void fraction is seen strongly by all the data presented for this study. Indeed, all the figures for this chapter are graphed with respect to quality. Plots of void fraction versus quality can be found in Figures 4.1, 4.4, 4.7, 4.10, 4.13, and 4.16. As can clearly be seen by these plots, an increase in quality results in an increase in void fraction. This makes sense, as quality is the ratio of vapor refrigerant to total refrigerant on a mass flow basis, while void fraction is the ratio of vapor refrigerant to total refrigerant on a volume basis.

4.1.2 Effect of Mass Flux on Void Fraction

In previous works on void fraction in condensation, Kopke (1998) and Graham (1997) found that mass flux had an effect on void fraction. The results of these studies showed that a lower mass flux showed a lower void fraction. Figure 4.4 shows the effect of mass flux on void fraction in the lower oil concentration range tested. A slight effect similar to that found by Kopke and Graham can be seen, that with lower mass fluxes the void fraction is lower, but is much less pronounced with this data. Figure 4.10 shows the void fraction results separated by mass flux, but here there is no extremely noticeable mass flux effect on void fraction. Thus, for this study, only the lower oil concentration levels appear to show a mass flux effect on void fraction.

4.1.3 Tube Type Effects on Void Fraction

Figures 4.1 and 4.7 show void fraction separated by tube type for the two oil concentrations tested. In the earlier works of Graham (1997), Kopke (1998), Wilson (1998), and Yashar (1998), the smooth tube type showed a higher void fraction than microfinned tubes at the same conditions. A similar trend was seen in this study, with the axial and helical sections showing a slightly lower void fraction at the same conditions than the smooth section. However, there was no clear trend differentiating the void fraction of the enhanced tube sections.

4.1.4 Oil Concentration Effects on Void Fraction

Figures 4.1, 4.7, 4.13, and 4.16 can be used to analyze the effects of oil concentration on void fraction. The void fraction and flowing oil concentration were determined by the techniques described in Chapter 3. The effect of the two oil concentration ranges tested can be determined by comparing Figures 4.1 and 4.7. However, there does not appear to be a difference in the void fraction between these two concentration ranges. Figures 4.13 and 4.16 show a breakdown of the oil concentration within the low and high oil concentration ranges, but these also show no clear effect of flowing oil concentration on void fraction.

4.2 Oil Holdup Results

The oil holdup results presented here were obtained using the methods outlined in Chapter 3. However, it should be noted that a number of experiments were conducted without the rinsing of the test sections to determine a base weight, and these results can be found in Appendix A. The oil holdup results will be broken up similar to the void fraction results, according to quality, mass flux, tube type, and oil concentration. The uncertainties in the oil holdup results ranged from approximately 25% in the lower oil concentration range to 5-12% in the higher oil concentration range.

4.2.1 Quality Effects on Oil Holdup

All the figures presenting oil holdup results are arranged versus quality, and can be found in figures 4.2, 4.5, 4.8, 4.11, 4.14, and 4.17. For the lower range of oil concentration tested (0.1-0.2 %), quality appears to have a definite effect on the oil holdup. As seen in Figures 4.2, 4.5, and 4.14, the overall mass of oil held up in the sections is very low. However, the amount of oil caught in the sections appears to be comparatively high in the low quality region, dip as the quality increases, and then increase again as the quality approaches one. However, there is not enough data in the low concentration range to define this trend further.

The higher oil concentration tested can be seen in Figures 4.8, 4.11, and 4.17. The amount of oil held up in these sections is much greater compared to the amount seen in the lower concentration range. This data shows a similar trend to the one discussed for the low concentration range. At low quality (0.1), the oil holdup is comparatively high, and then dips as the quality increases to around 0.7. As the quality increases from this point to approach an all vapor flow, the amount of oil held in the test sections increases. Thus, the oil holdup appears to follow a trend with a low point in the mid-quality range (0.3-0.7), with comparatively higher holdups in the low (0.1) and high quality (0.8-0.95) ranges tested.

4.2.2 Mass Flux Effects on Oil Holdup

Figures 4.5 and 4.11 show the oil holdup versus quality results for this study, separated by mass flux. However, the data shown appear to be fairly well mixed and show no clear differentiation based on mass flux.

4.2.3 Tube Type Effects on Oil Holdup

The effect of tube geometry can be seen in Figures 4.2 and 4.8. Figure 4.2 show s the data for the low concentration range tested, which does not suggest a clear trend in oil holdup based on tube geometry. However, the data range on this graph is fairly small, so clearly observing trends is somewhat difficult.

Figure 4.8 shows the higher oil concentration range tested arranged with regard to tube geometry. This data appears to show a slight trend of the smooth test section holding up slightly less oil. However, this trend appears to be very slight, and is within the 5-10 percent uncertainty range seen in the high oil holdup data.

4.2.4 Oil Concentration Effects on Oil Holdup

Figures 4.14 and 4.17 show the tow concentration ranges tested broken down amongst themselves. By comparing these two graphs, it is obvious that very little oil is held up at the low concentration range, with the amounts held up being less than 0.1 g/m. The higher oil concentration range locally leads to much higher oil holdup, up to slightly less than 1.6 g/m.

The data shown in Figure 4.14 does not show a clear trend in oil holdup in the 0.1-0.2 % oil concentration range. While some of the highest holdups are recorded near the high end of this range, there are several points in the

high end of the oil concentration range where no oil is held up in the section. Therefore, at the low oil concentration range tested, the flowing oil concentration does not have a clear effect on the amount of oil held up in the section.

Figure 4.17 shows the oil concentration effects on oil holdup for the 2-4 % oil range. This graph appears to show that at the higher oil range, variations in the flowing oil concentration can result in changes in the amount of oil held up in the test sections. The trend this figure shows is a logical one, that as the oil concentration increases, the amount of oil held up in the test section increases slightly as well.

4.3 Slip Ratio Results

The slip ratio results were calculated as detailed in Chapter 2. The slip ratio was calculated from the experimentally determined void fraction.

4.3.1 Quality Effects on Slip Ratio

Figures 4.3, 4.6, 4.9, 4.12, 4.15, 4.18 all show the calculated slip ratios plotted versus quality. All of these plots show a trend of slip ratio slowly increasing linearly with quality until a quality of approximately 0.7, at which point the slip ratio increases very quickly with quality. This makes sense, since the slip ratio is the ratio of the vapor to liquid speeds, and as more of the mass flow is due to the less dense vapor, the vapor velocity increases.

4.3.2 Mass Flux Effects on Slip Ratio

Figures 4.6 and 4.12 show slip ratio plotted versus quality, separated by mass flux for the experiments conducted. However, there appears to be no trends in the data due to mass flux, with all the pints being mixed together.

4.3.3 Tube Type Effects on Slip Ratio

Figures 4.3 and 4.9 show the slip ratio results sorted by tube type. Figure 4.9 shows that at qualities of 0.7-1, there is a slight tube geometry effect on slip ratio. These results show that the smooth test section tended to show a lower slip ratio at a given set of conditions than did the microfinned tubes. Figure 4.3 shows a similar trend, but slightly less pronounced, partially due to its smaller data set. Thus, the enhanced tube sections show higher slip ratios at the mid to high quality range.

4.3.4 Oil Concentration Effects on Slip Ratio

Figures 4.3 and 4.9 can be used to compare the slip ratio in the low and high oil concentration ranges. However, upon comparing these two graphs, the values of the calculated slip ratio appear to be effected by the oil concentration range. Thus, the amount of oil floating in the loop did not appear to effect the slip ratio.

Figures 4.15 and 4.17 show the slip ratio differentiated by the oil concentration variations within the tested ranges. However, there appears to be no systematic trend in the slip ratio as the oil concentration changes within each individual range.

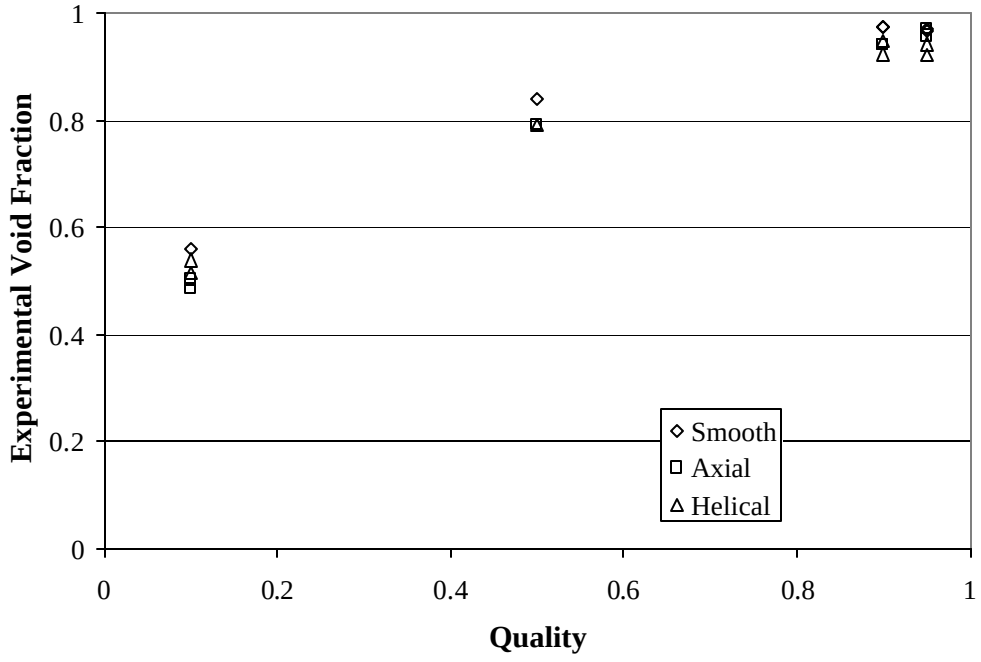

Figure 4.1: Experimental Void Fraction vs. Quality for R134a/ 0.1-0.2 % ISO 32 POE, with rinsing, separated by tube type

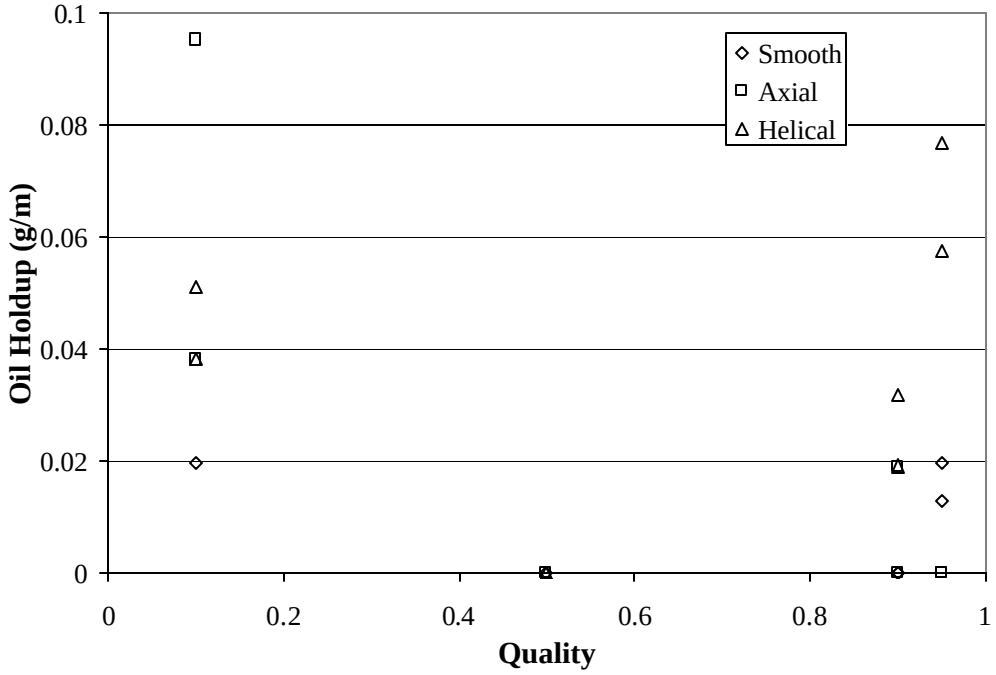

Figure 4.2: Oil Holdup vs. Quality for R134/0.1-0.2 % ISO 32 POE, with rinsing, separated by tube type

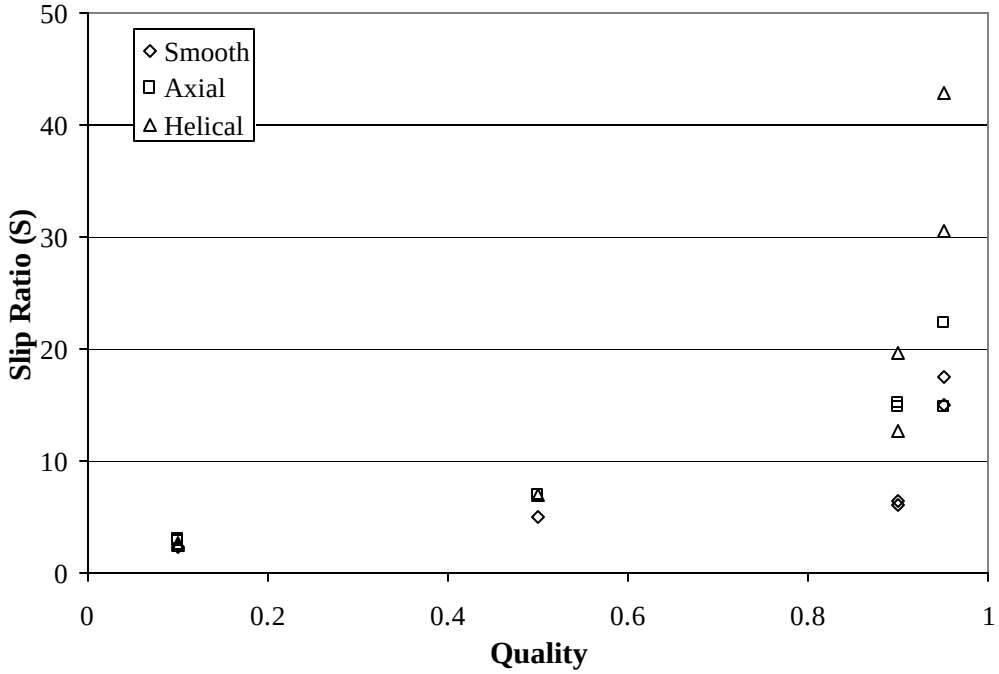

Figure 4.3: Slip Ratio vs. Quality for R134/0.1-0.2 % ISO 32 POE, with rinsing, separated by tube type

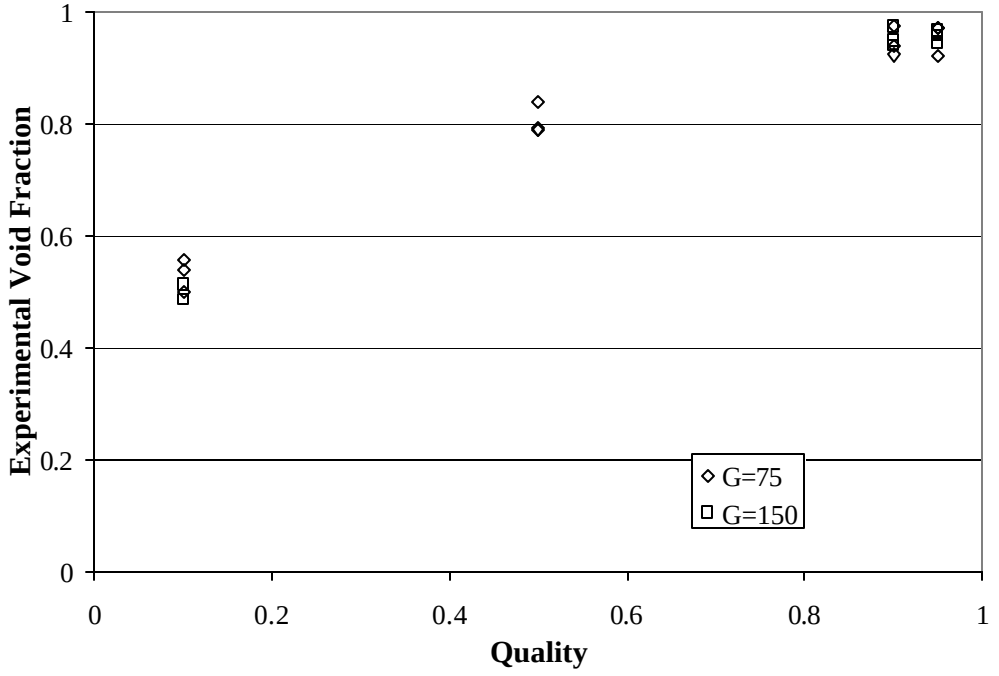

Figure 4.4: Experimental Void Fraction vs. Quality for R134/ 0.1-0.2% ISO 32 POE, with rinsing, separated by mass flux

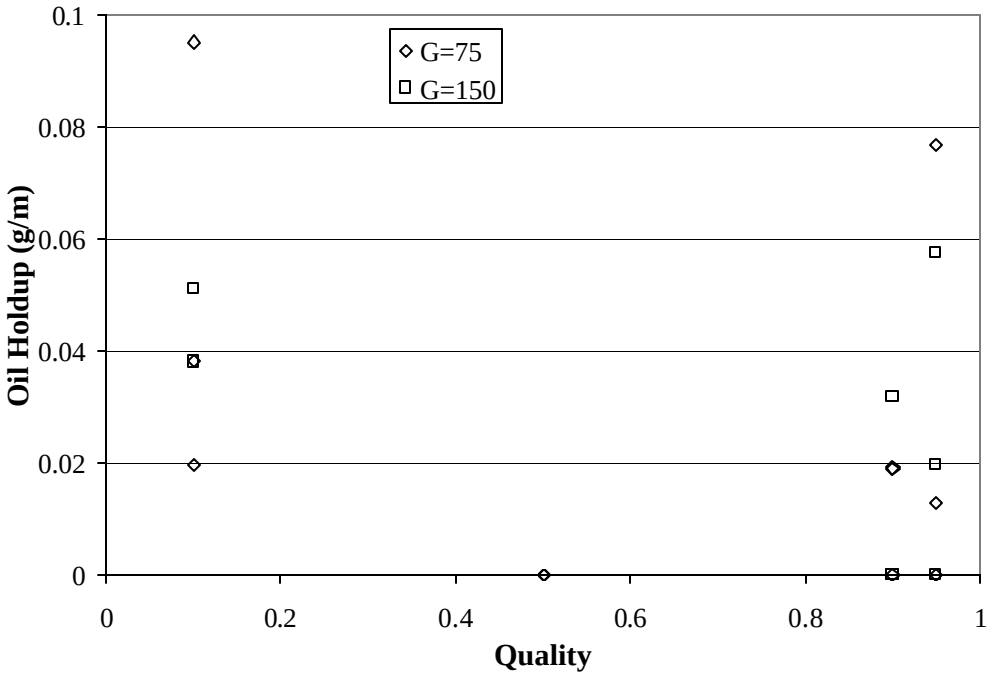

Figure 4.5: Oil Holdup vs. Quality for R134/ 0.1-0.2% ISO 32 POE, with rinsing, separated by mass flux

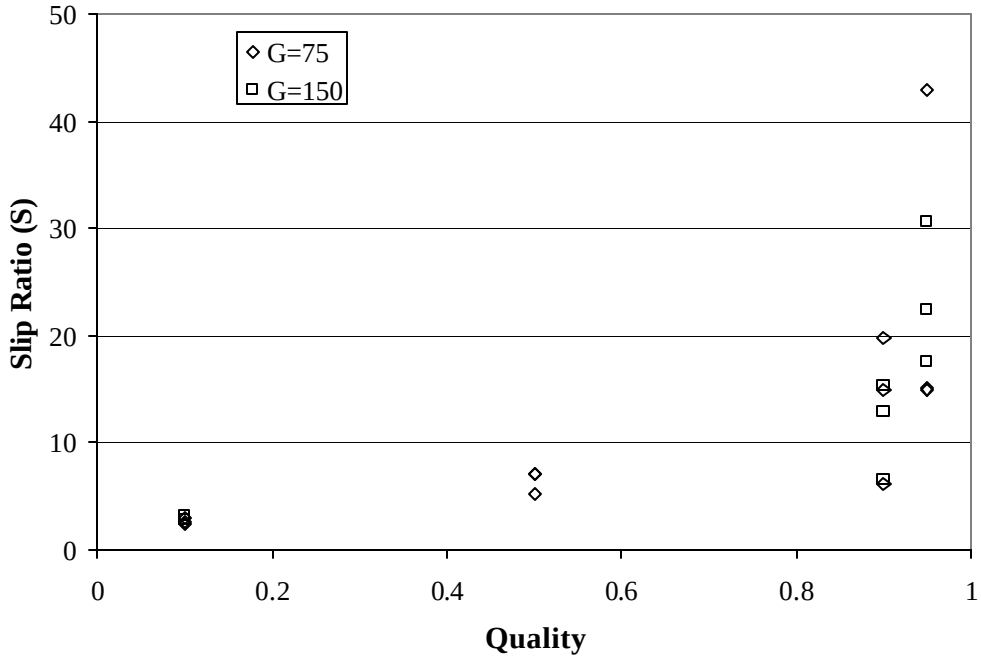

Figure 4.6: Slip Ratio vs. Quality for R134a/ 0.1-0.2 % ISO 32 POE, with rinsing, separated by mass flux

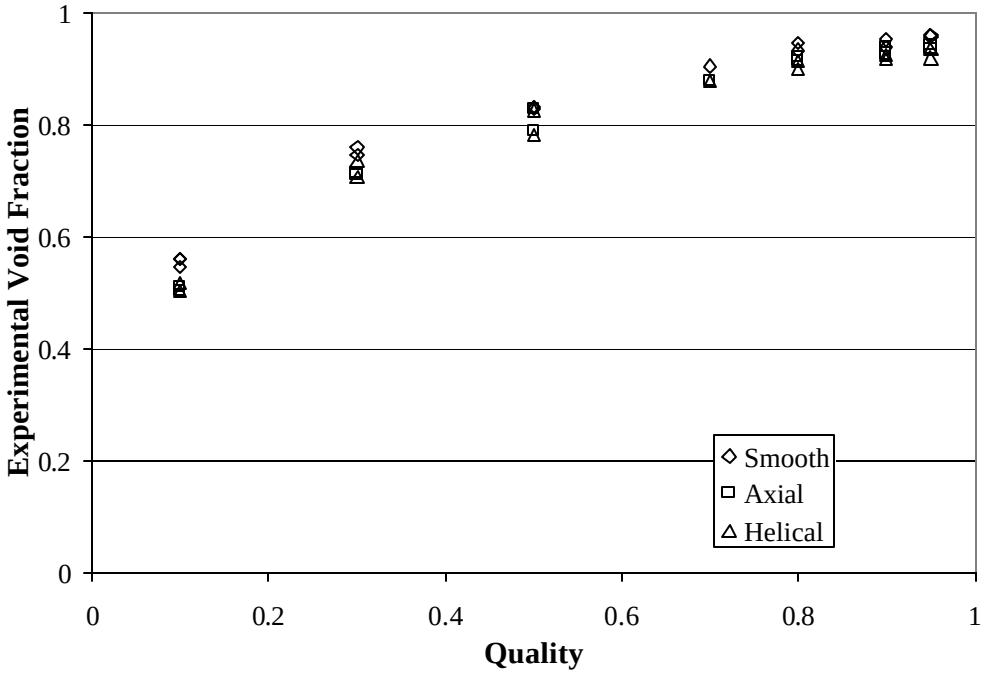

Figure 4.7: Experimental Void Fraction vs. Quality for R134/ 2-4 % ISO 32 POE, with rinsing, separated by tube type

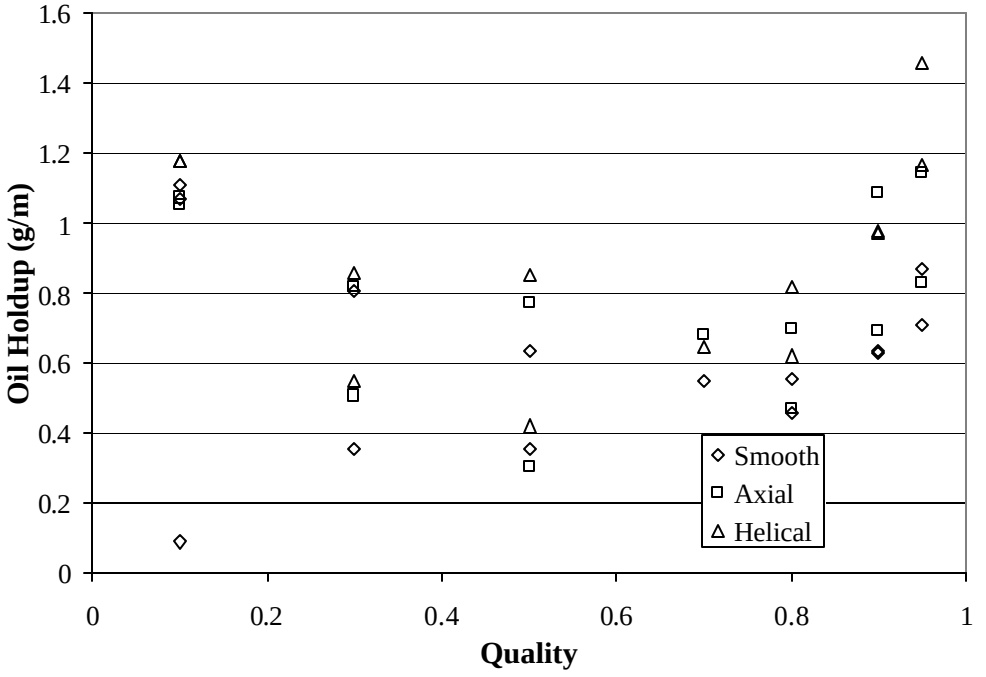

Figure 4.8: Oil Holdup vs. Quality for R134/ 2-4 % ISO 32 POE, with rinsing, separated by tube type

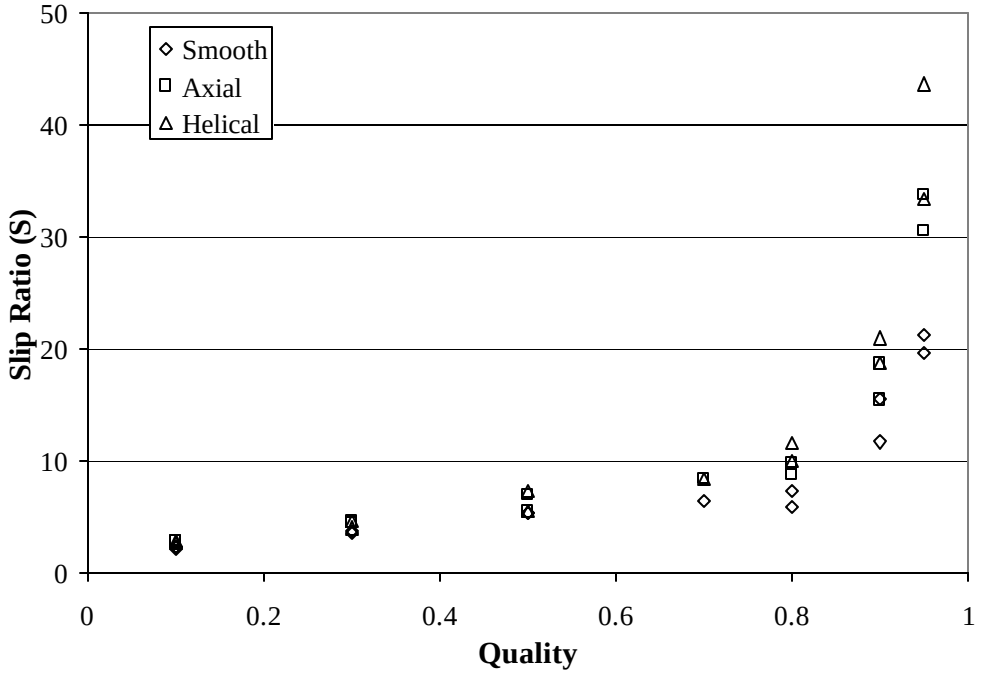

Figure 4.9: Slip Ratio vs. Quality for R134/ 2-4 % ISO 32 POE, with rinsing, separated by tube type

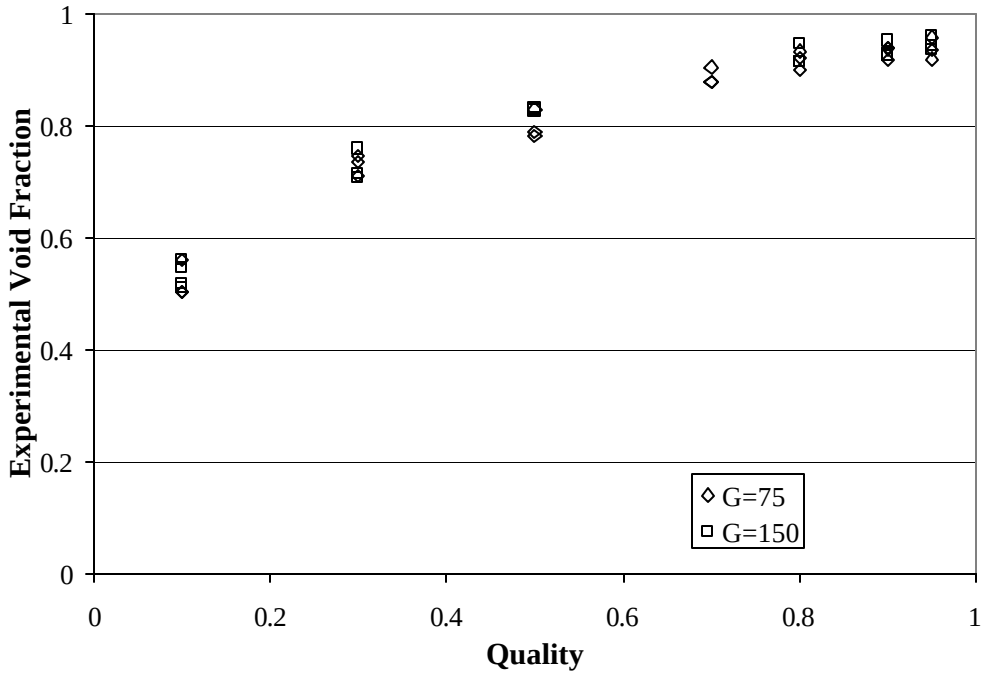

Figure 4.10: Experimental Void Fraction vs. Quality for R134/ 2-4 % ISO 32 POE, with rinsing, separated by mass flux

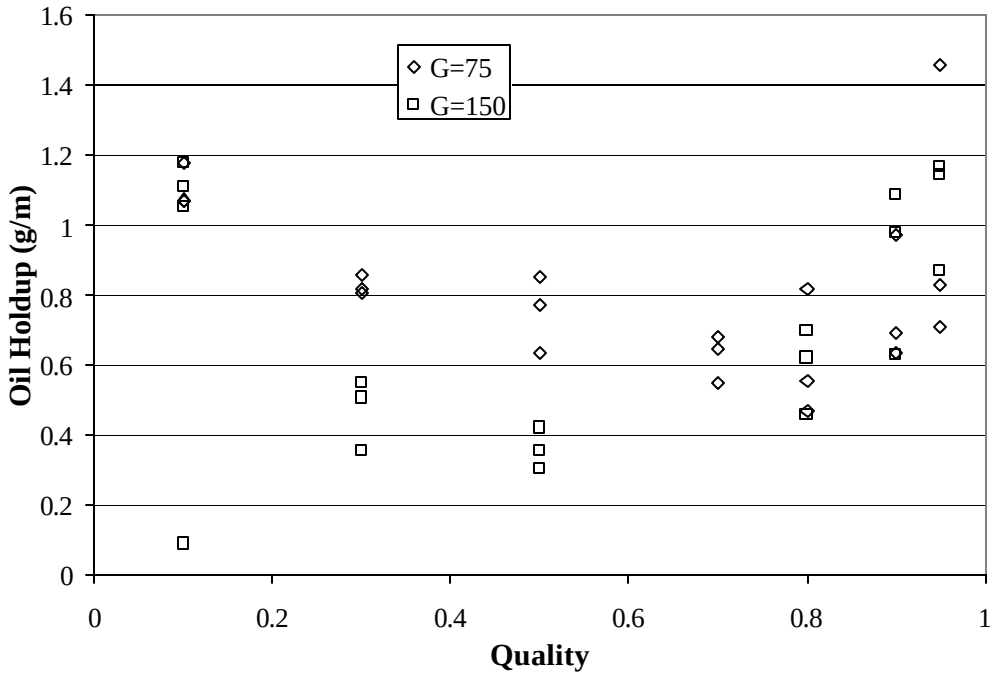

Figure 4.11: Oil Holdup vs. Quality for R134/ 2-4 % ISO 32 POE, with rinsing, separated by mass flux

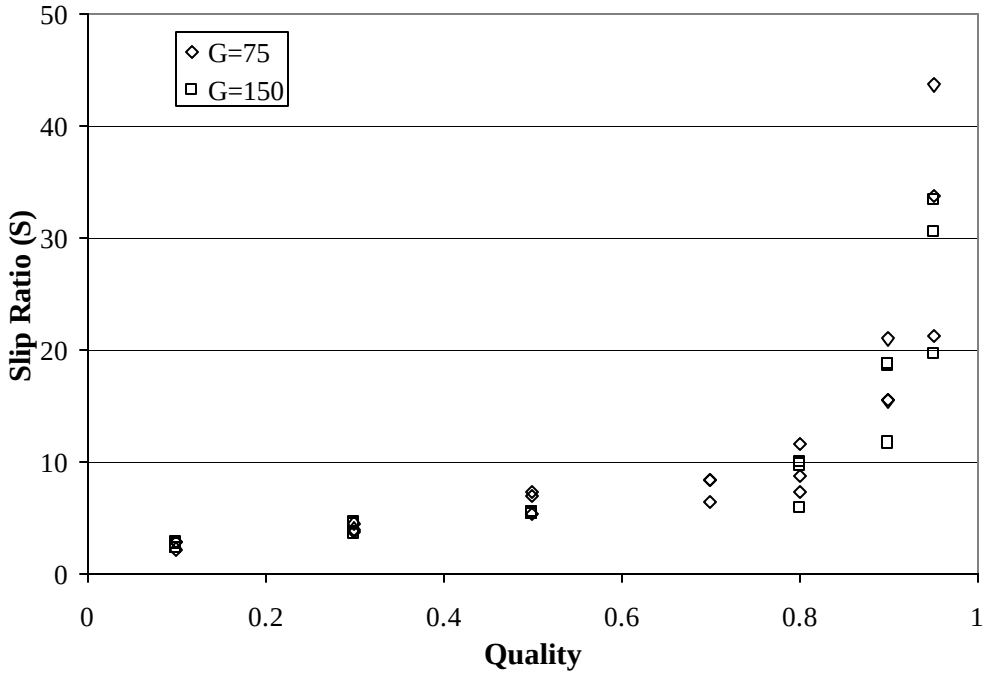

Figure 4.12: Slip Ratio vs. Quality for R134/ 2-4 % ISO 32 POE, with rinsing, separated by mass flux

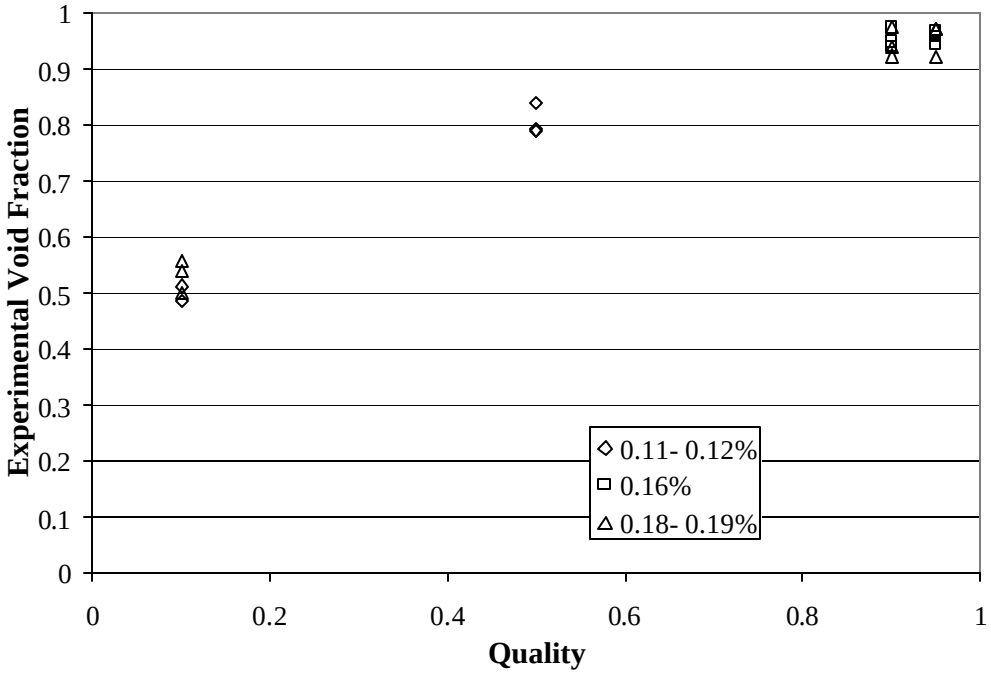

Figure 4.13: Experimental Void Fraction vs. Quality for R134/ 0.1-0.2 % ISO 32 POE, with rinsing, separated by oil concentration

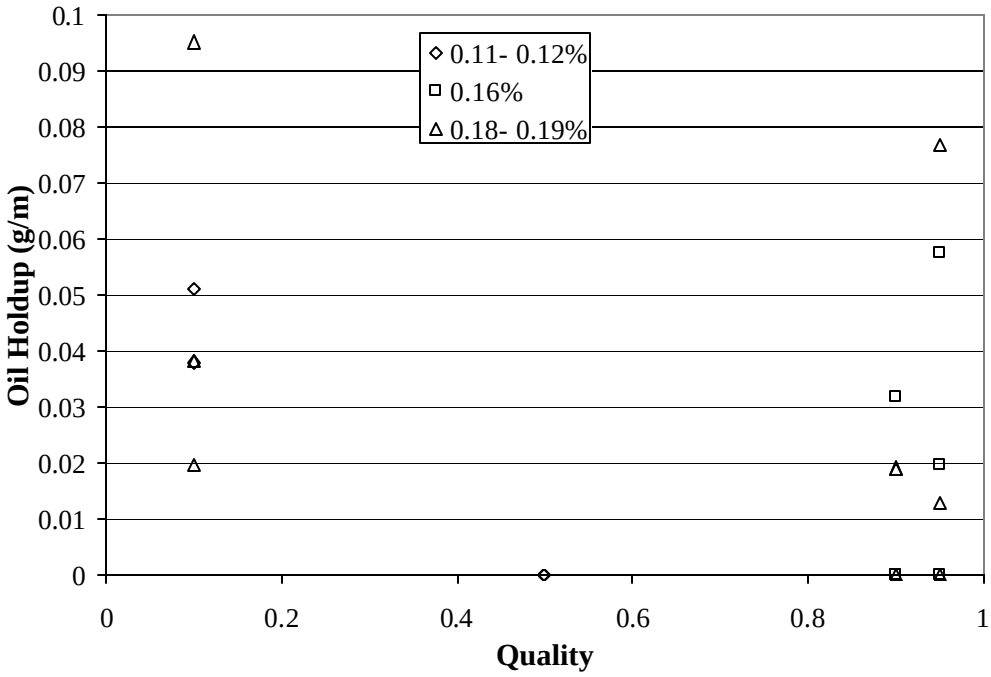

Figure 4.14: Oil Holdup vs. Quality for R134/ 0.1-0.2 % ISO 32 POE, with rinsing, separated by oil concentration

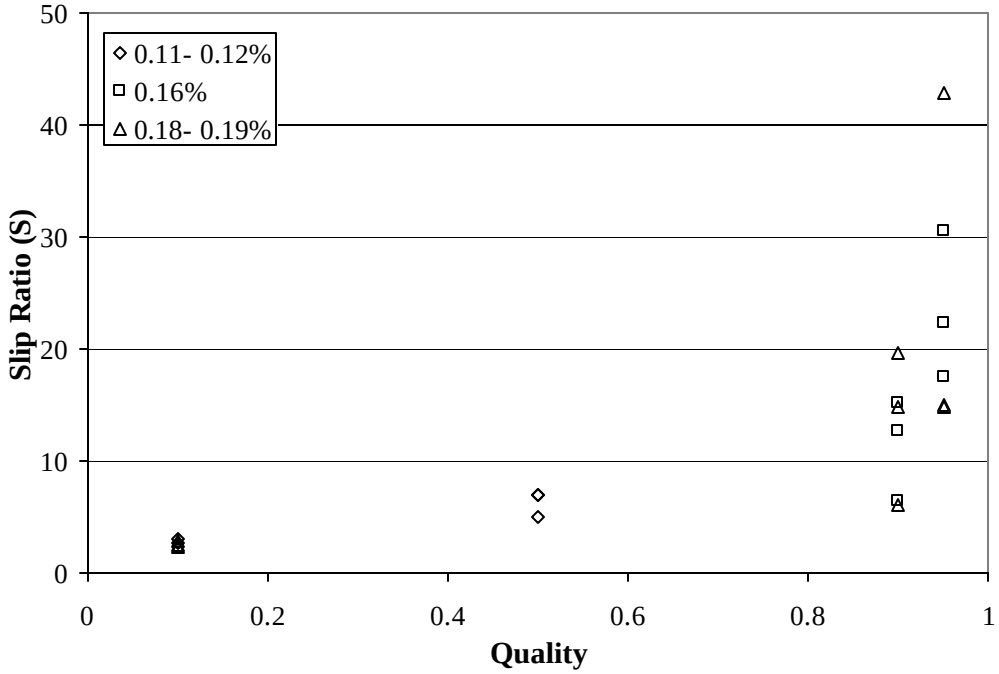

Figure 4.15: Slip Ratio vs. Quality for R134/ 0.1-0.2 % ISO 32 POE, with rinsing, separated by oil concentration

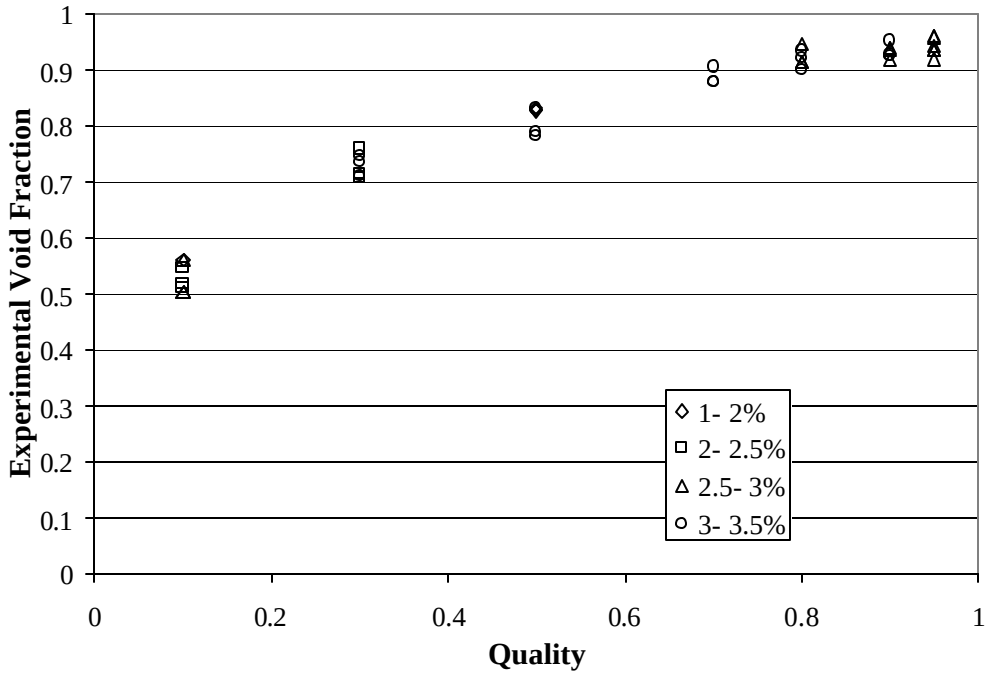

Figure 4.16: Experimental Void Fraction vs. Quality for R134/ 2-4 % ISO 32 POE, with rinsing, separated by oil concentration

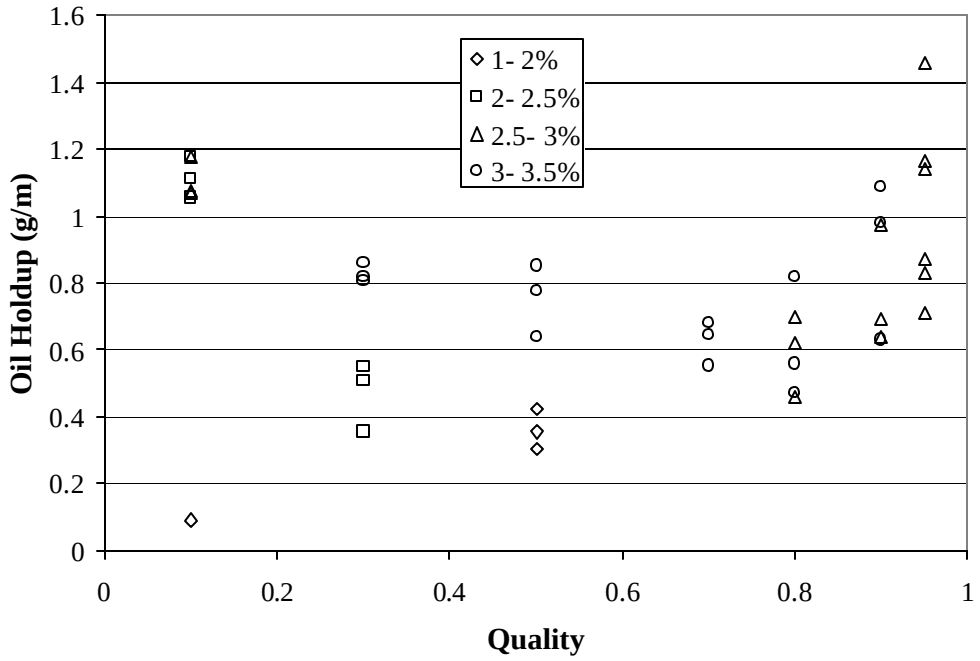

Figure 4.17: Oil Holdup vs. Quality for R134/ 2-4 % ISO 32 POE, with rinsing, separated by oil concentration

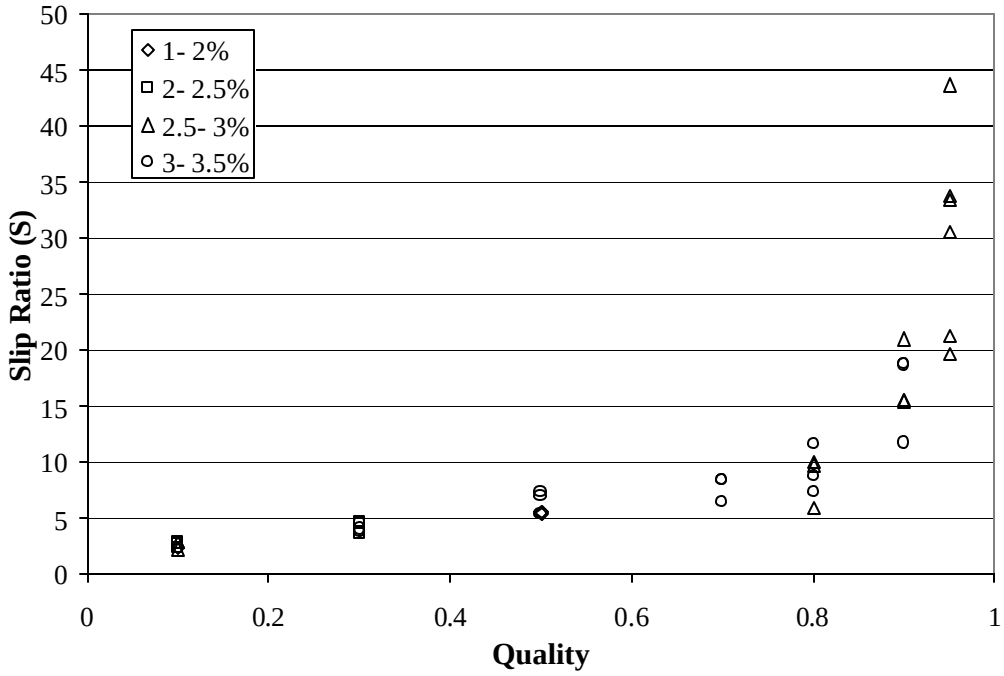

Figure 4.18: Slip Ratio vs. Quality for R134/ 2-4 % ISO 32 POE, with rinsing, separated by oil concentration

Chapter 5: Analysis of Data

This chapter consists of the analysis of the data collected in this study, and its comparison to existing correlations. Some of the different models used for determining liquid viscosity of the refrigerant-oil mixtures will be used to compare with the void fraction experimental results. Also, modeling of the oil holdup will be discussed.

5.1 Void Fraction Analysis

The experimental void fraction data was compared to the void fraction predicted by the ACRC void fraction model referenced in Chapter 2. These results can be seen in Figures 5.1- 5.3. These figures include both oil concentration regions, are arranged by tube type, and include lines to signify +/- 10 % agreement between the model and experimental data. Also, the viscosity values used for the liquid refrigerant/ oil mixtures, including pure refrigerant data, as well as the linear, Baustian, and Cawte models referenced in Chapter 2 separate the data. Appendix C lists the output of all these models, as well as their respective errors compared to the experimental data. The figures show very little variation in the predicted void fraction as the viscosity model is changed. Thus, there appears to be very little advantage to adjusting the liquid void fraction due to the addition of oil at the ranges tested in this study. These results indicate that refrigerant charge prediction should be relatively insensitive to oil for the concentration and viscosity range tested.

5.2 Oil Holdup Results

The oil holdup results were compared to a model derived from a conservation of mass analysis. This model starts out by calculating the amount of oil in the tube at the measured flowing oil concentration if the flow fills the test section and is entirely liquid, as seen in equation 5.1. That amount is then used to predict the amount held up at a given flow quality and void fraction, as seen in equation 5.2.

$$m_o = c_o ?_l V_{ts} \tag{5.1}$$

$$m_{ox} = m_o \left(\frac{1-a}{1-x} \right) \tag{5.2}$$

The results of this comparison can be seen in figures 5.4- 5.10. Figures 5.4- 5.6 separate the results by tube type, and show no clear correlation between predicted values and tube type. Figures 5.7- 5.10 separate the data by mass flux, and also show no clear trends in mass flux effect on the oil holdup model. However, figures 5.4, 5.5, 5.7, and 5.8 include lines to show agreement of the predicted and experimental values to within +/- 10%. As can be seen in these results, the oil holdup model gives a rough idea of oil holdup at the higher flowing concentration range tested, but does not agree well with the data in the lower oil concentration range. This lack of agreement could very likely be due to a variety of factors, most likely of these being the uncertainty in the oil holdup measurements in this range, but also possibly the miscibility of the oil with the refrigerant leading to small amounts of holdup in the loop. Thus, using the conservation of mass model can provide an idea of oil holdup in tubes during higher (2-4%) oil concentration ranges, however it significantly overpredicts holdup at low (0.2- 0.4 %) concentration ranges in the mid-quality range.

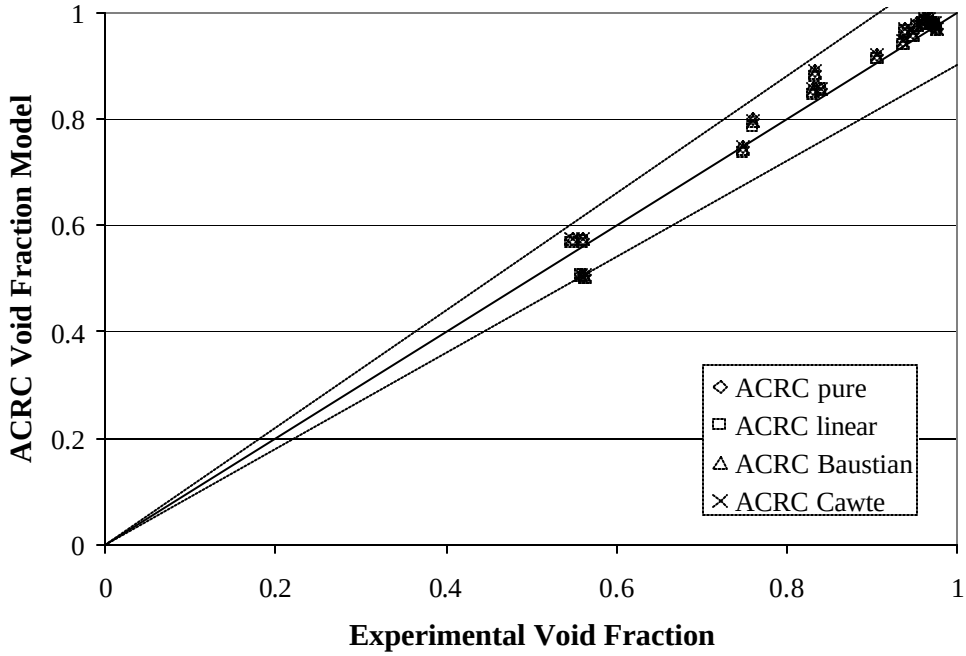

Figure 5.1: ACRC Void Fraction Model vs. Experimental Void Fraction for all oil concentrations, with rinsing, smooth test section, separated by oil models

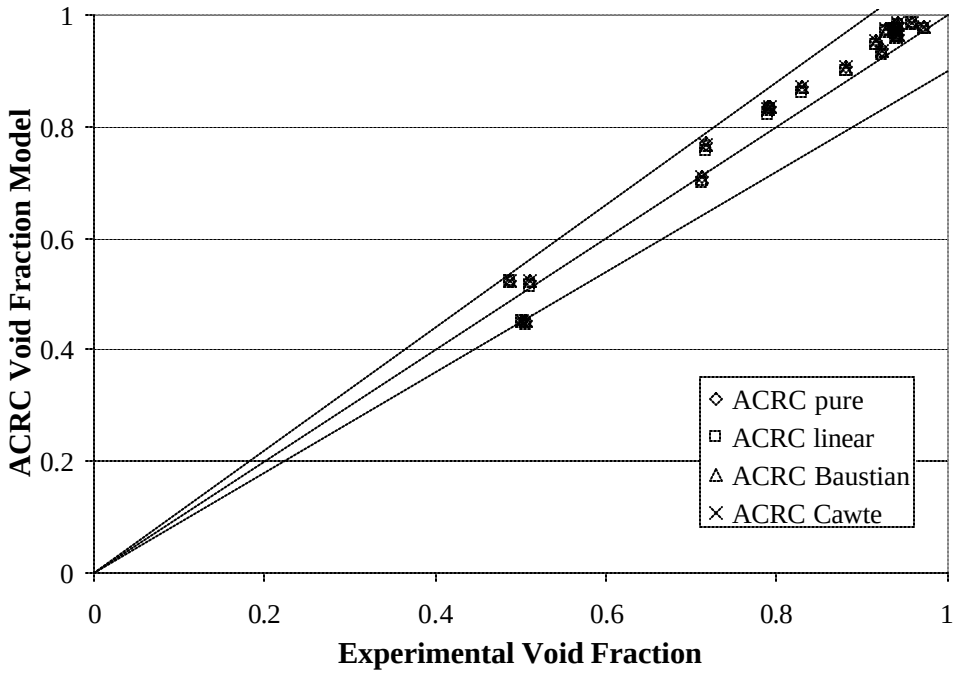

Figure 5.2: ACRC Void Fraction Model vs. Experimental Void Fraction for all oil concentrations, with rinsing, axial test section, separated by oil models

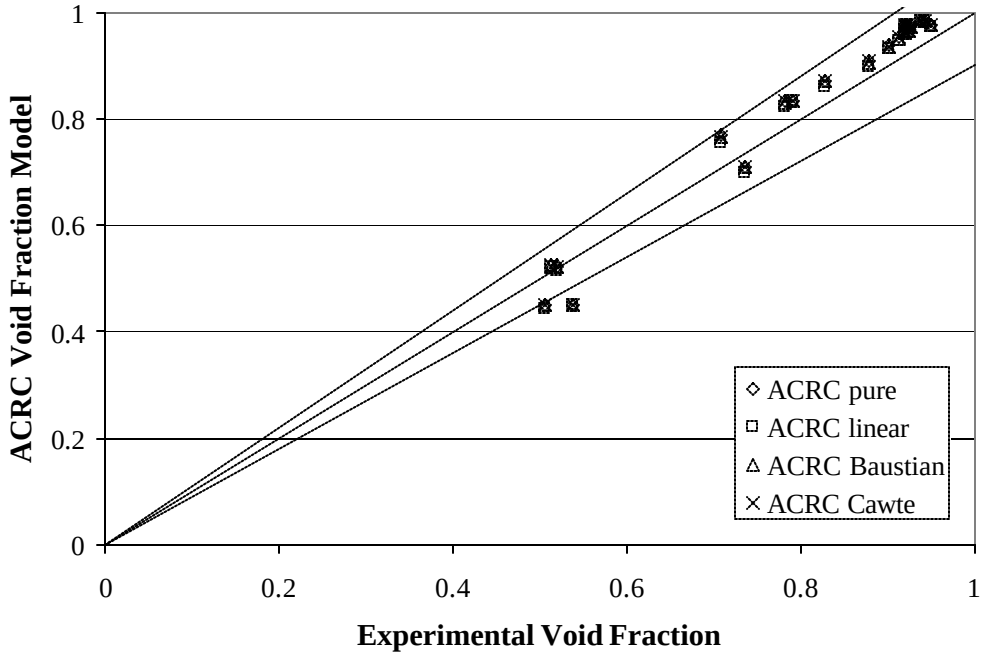

Figure 5.3: ACRC Void Fraction Model vs. Experimental Void Fraction for all oil concentrations, with rinsing, helical test section, separated by oil models

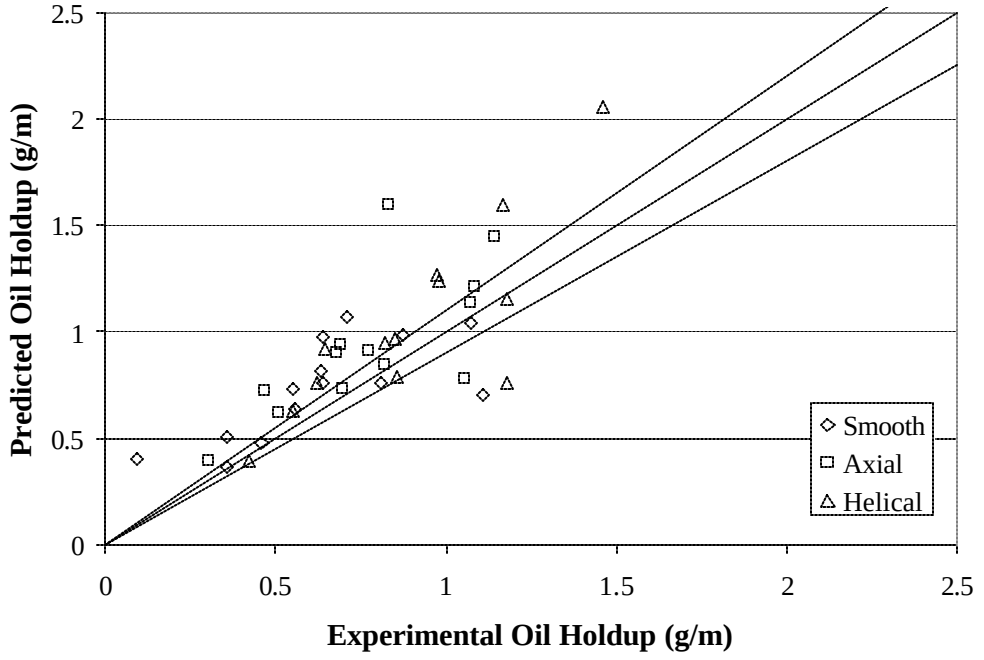

Figure 5.4: Predicted Oil Holdup (g/m) vs. Experimental Oil Holdup (g/m) for R134a/ 2-4 % ISO 32 POE, separated by tube type

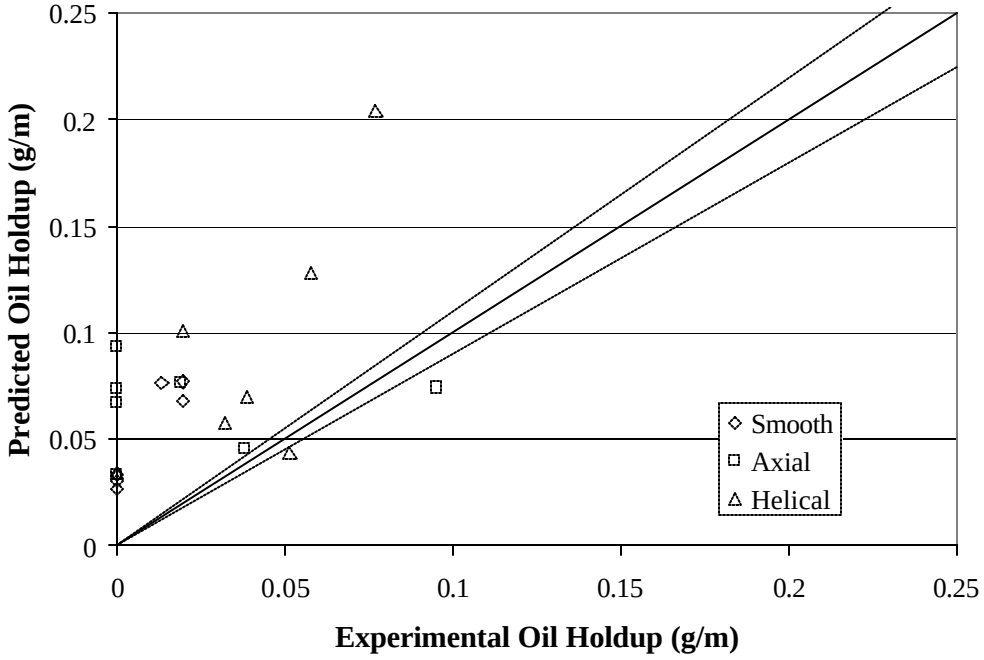

Figure 5.5: Predicted Oil Holdup (g/m) vs. Experimental Oil Holdup (g/m) for R134a/ 0.2-0.4 % ISO 32 POE, separated by tube type

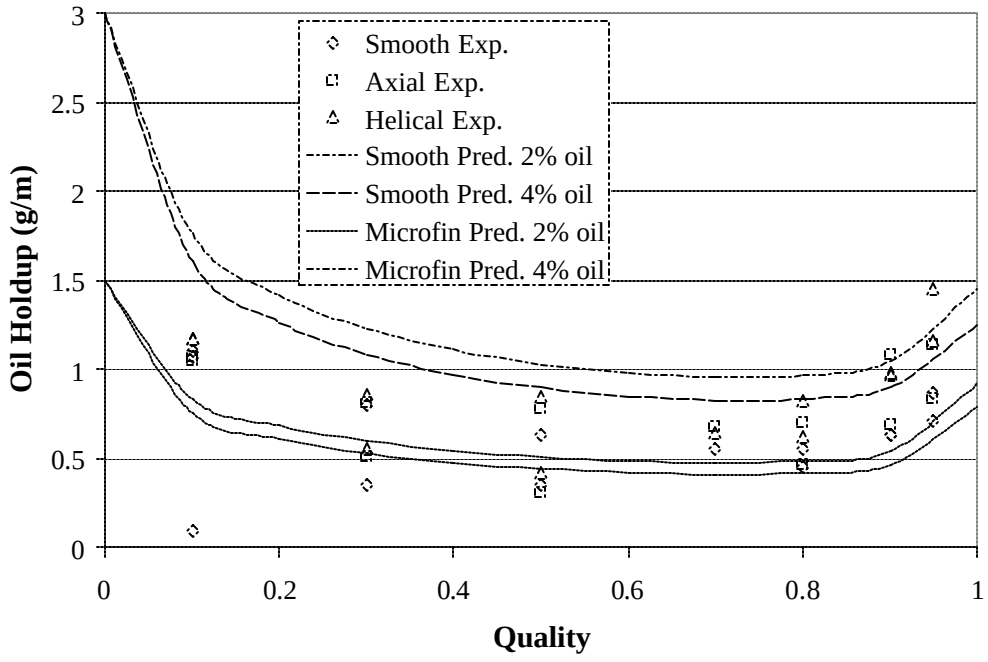

Figure 5.6: Oil Holdup (g/m) vs. Quality for R134a/ 2-4% ISO 32 POE, separated by tube type and predicted/ experimental data

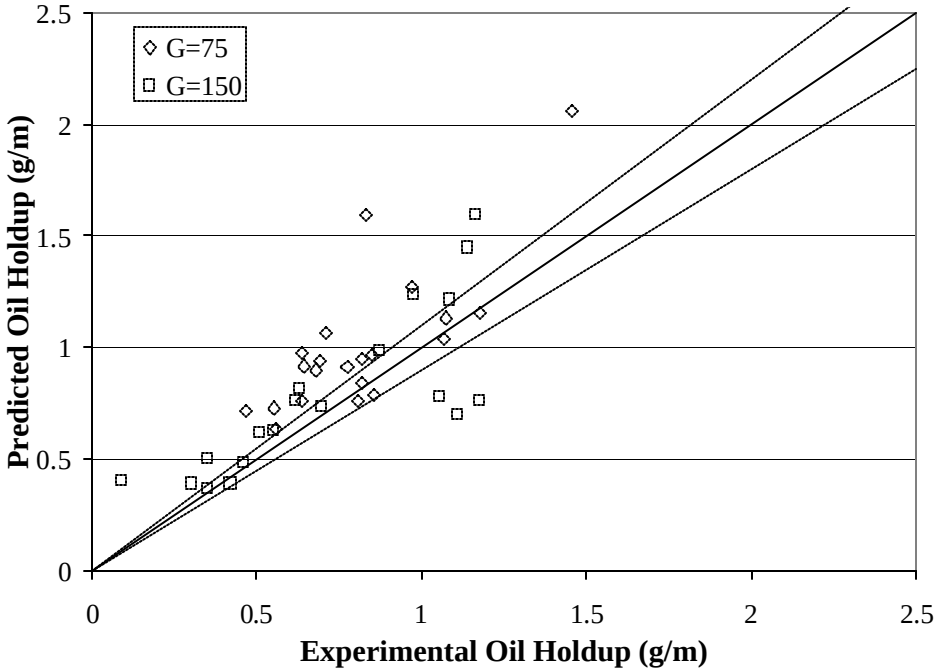

Figure 5.7: Predicted Oil Holdup (g/m) vs. Experimental Oil Holdup (g/m) for R134a/ 2-4 % ISO 32 POE, separated by mass flux

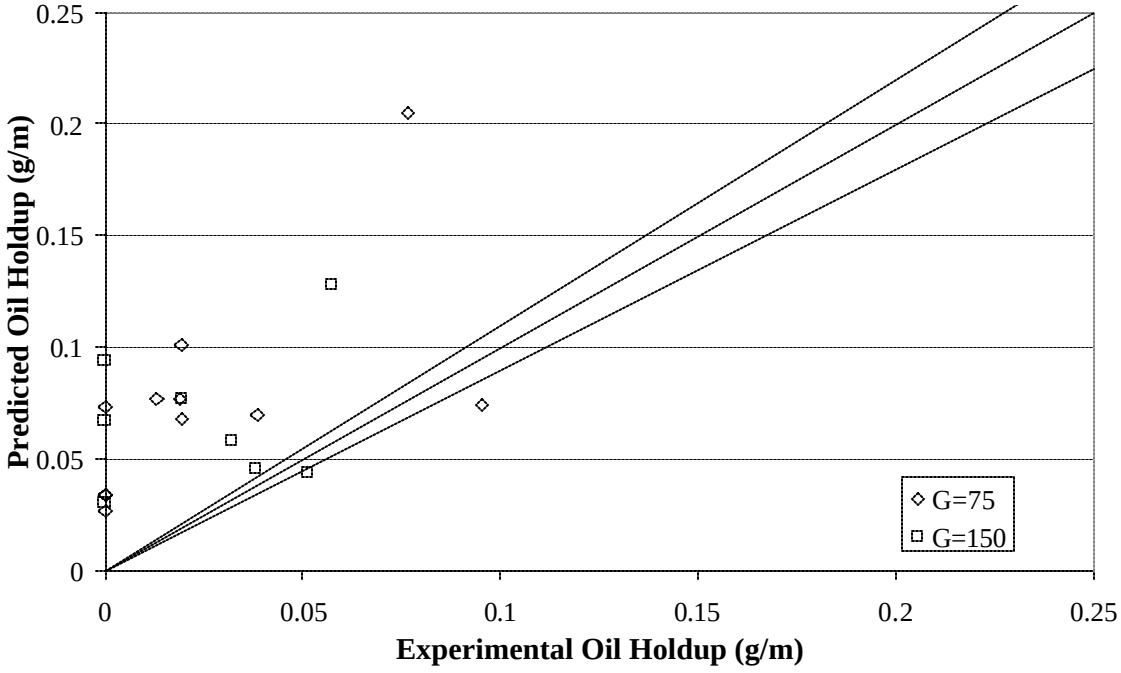

Figure 5.8: Predicted Oil Holdup (g/m) vs. Experimental Oil Holdup (g/m) for R134a/ 0.2-0.4 % ISO 32 POE, separated by mass flux

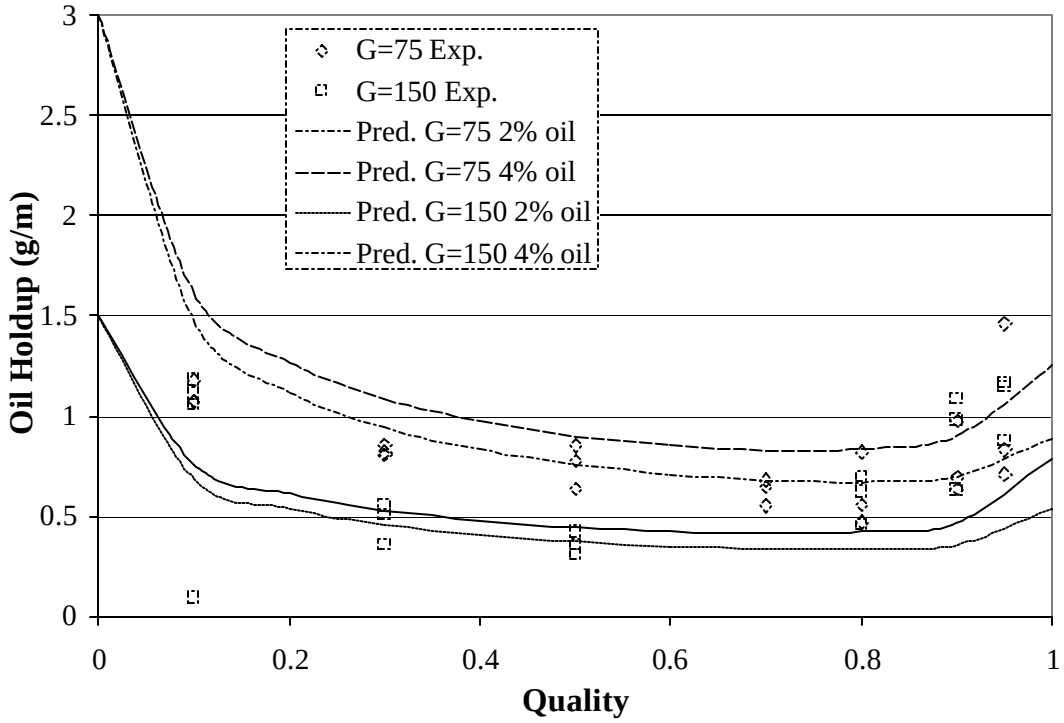

Figure 5.9: Oil Holdup (g/m) vs. Quality for R134a/ 2-4% ISO 32 POE, separated by mass flux and predicted/ experimental data

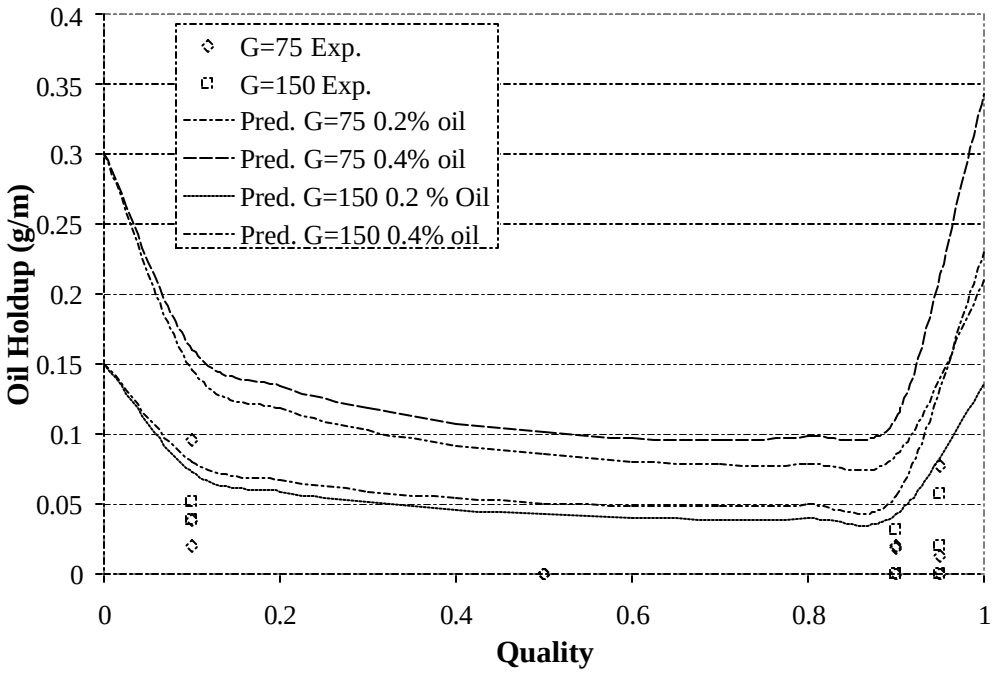

Figure 5.10: Oil Holdup (g/m) vs. Quality for R134a/ 0.2-0.4% ISO 32 POE, separated by mass flux and predicted/ experimental data

Chapter 6: Conclusion

This study examined the effects of oil when mixed with refrigerant upon system properties. Specifically, this study examined experimental data obtained with R134a refrigerant and ISO 32 polyol ester oil for void fraction and oil holdup in horizontal tubes. The void fraction, which can be used to predict charge, was found to be relatively unaffected by the addition of up to 4% oil, so the addition of oil did not seem to effect the amount of refrigerant needed to run a condenser effectively. Oil holdup, however, had varying trends in the low and high concentrations tested (0.2-0.4 and 2-4 mass %, respectively). In the lower oil concentration range, very little oil was found to be held up in the test sections. However, in the higher range, this holdup increased, and showed a noticeable trend. It was found that this trend could be predicted by using a model based on conservation of mass, as explained in Chapter 5. Also, the end points for oil holdup prediction can be based at the liquid end of the two phase region by using the amount of oil held up in a fully liquid flow, while at the high end by a law of the wall analysis using pure vapor refrigerant flow with an oil film. Thus, trends in void fraction and oil holdup were determined by this study.

Bibliography

Baroczy, C. J, "Correlation of liquid fraction in two-phase flow with application to liquid metals", *Chemical Engineering Progress Symposium Series*, Vol. 61, No. 57, pp. 179-191, 1965.

Baustian, J. J., M. B. Pate, and A.E. Bergles, "Properties of Oil-Refrigerant Mixtures with Applications to Oil Concentration Measurement: Part I—Thermophysical and Transport Properties," *ASHRAE Transactions*, Vol.92, part 1, pp.55-73, 1986.

Cawte, H., D.A. Sanders, and G.A. Poland, "Effect of Lubricating Oil Contamination on Evaporation in Refrigerants R12 and R22," *International journal of Energy Research*, Vol.20, pp. 663-679, 1996.

Dobson, M.K., "Heat transfer and flow regimes during condensation in a horizontal tube", Ph.D. Dissertation, University of Illinois, 1994.

Domanski, P., and D. Didion. *Computer Modeling of the Vapor Compression Cycle with Constant Flow Area Expansion Device*. NBS Building Science Series 155, 1983.

F-Chart Software. "Engineering Equation Solver (EES)", version 6.036. Computer software. 2000.

Gaibel, J.A., J.C. Chato, M.K. Dobson, M. Ponchner, P.J. Kenney, R.L.. Shimon, T.C. Villaneuva, N.L. Rhines, K.A. Sweeney, D.G. Allen, and T.T. Hershberger. "Condensation of a 50/50 Blend of R-32/R-125 in Horizontal Tubes With and Without Oil," ACRC TR-56, Air Conditioning andRefrigeration Center, University of Illinois, Urbana-Champaign IL, 1994.

Graham, D.M, T.A. Newell and J.C. Chato, "Experimental Investigation of Void Fraction During Refrigerant Condensation", ACRC TR-144, Air Conditioning and Refrigeration Center, University of Illinois, Urbana-Champaign IL, 1998(a).

Graham, D.M., H.R. Kopke, M.J. Wilson, D.A. Yashar, J.C. Chato, and T.A. Newell "An Investigation of Void Fraction in the Annular/Stratified Flow Regions in Smooth, Horizontal Tubes", ACRC TR-144, Air Conditioning and Refrigeration Center, University of Illinois, Urbana-Champaign IL, 1998(b).

Harms, T.M., "Charge Inventory Modeling and Validation for Unitary Heat Pumps," Preliminary Report, Purdue University, 2001.

Hurlbert, E.T., and T.A. Newell, "Modeling of the Evaporation and Condensation of Zeotropic Refrigerant Mixtures in Horizontal, Annular Flow", ACRC TR-129, Air Conditioning and Refrigeration Center, University of Illinois, Urbana-Champaign IL, 1997.

Incropera, F.P. and D.P. Dewitt, *Fundamentals of Heat and Mass Transfer*, 4th edition, Wiley, New York, 1996.

Kopke, H.R., T.A. Newell, and J.C. Chato, "Experimental Investigation of Void Fraction during Refrigerant Mixtures in Horizontal Tubes", ACRC TR-142, Air Conditioning and Refrigeration Center, University of Illinois, Urbana-Champaign IL, 1998.

Lockhart, R. W. and R. C. Martinelli. "Proposed correlation of data for isothermal two-phase, two-component flow in pipes." *Chemical Engineering Progress*, Vol. 45, No. 1, pp. 39-48, 1949.

Reid, Robert C., John M. Prausnitz, and Bruce E. Poling, *The Properties of Gases & Liquids*, Fourth Edition. McGraw-Hill Inc., United States, 1986.

Rice, C.K, "The effect of void fraction correlation and heat flux assumption on refrigerant charge inventory predictions." *ASHRAE Transactions*, Vol. 93, Part 1, pp. 341-367, 1987.

Sacks, P.S. "Measured characteristics of adiabatic and condensing single-component two-phase flow of refrigerant in a 0.377 in. diameter horizontal tube. *ASME Winter Annual Meeting*, Houston, TX, 75-WA/HT-24.

Smith, S. L. "Void fractions in two-phase flow: a correlation based upon an equal velocity head model." *Proc. Instn. Mech Engrs.*, London, Vol. 184, Pt. 1, No. 36, pp. 647-664, 1969.

Tichy, J.A., N.A. Macken, and W.M.B. Duval, "An Experimental Investigation of Heat Transfer in Forced Convection Condensation of Oil-Refrigerant Mixtures," *ASHRAE Transactions*, Vol.91, Part 1A, pp.297-303, 1985.

Wallis, G. B. *One-Dimensional Two-Phase Flow*. New York: McGraw-Hill, pp. 51-54, 1964.

Wilson, M.J., T.A. Newell, and J.C. Chato. “Experimental Investigation of Void Fraction during Horizontal Flow in Larger Diameter Refrigeration Applications”. ACRC TR-140, Air Conditioning and Refrigeration Center, University of Illinois, Urbana-Champaign IL, 1998.

Yashar, D.A., T.A. Newell, and J.C. Chato. “Experimental Investigation of Void Fraction during Horizontal Flow in Smaller Diameter Refrigeration Applications”. ACRC TR-141, Air Conditioning and Refrigeration Center, University of Illinois, Urbana-Champaign IL, 1998.

Yashar, D.A., M.J. Wilson, H.R. Kopke, D.M. Graham, J.C. Chato, and T.A. Newell, “An Investigation of Refrigerant Void Fraction in Horizontal, Microfin Tubes”, *International Journal of HVAC&R Research*, to appear, 2001.

Zivi, S. M. 1964. "Estimation of steady-state steam void-fraction by means of the principle of minimum entropy production." *Transactions ASME, Journal of Heat Transfer*, Series C, Vol. 86, May, pp. 247-252.

Appendix A: Figures and Data for Experiments without Rinsing

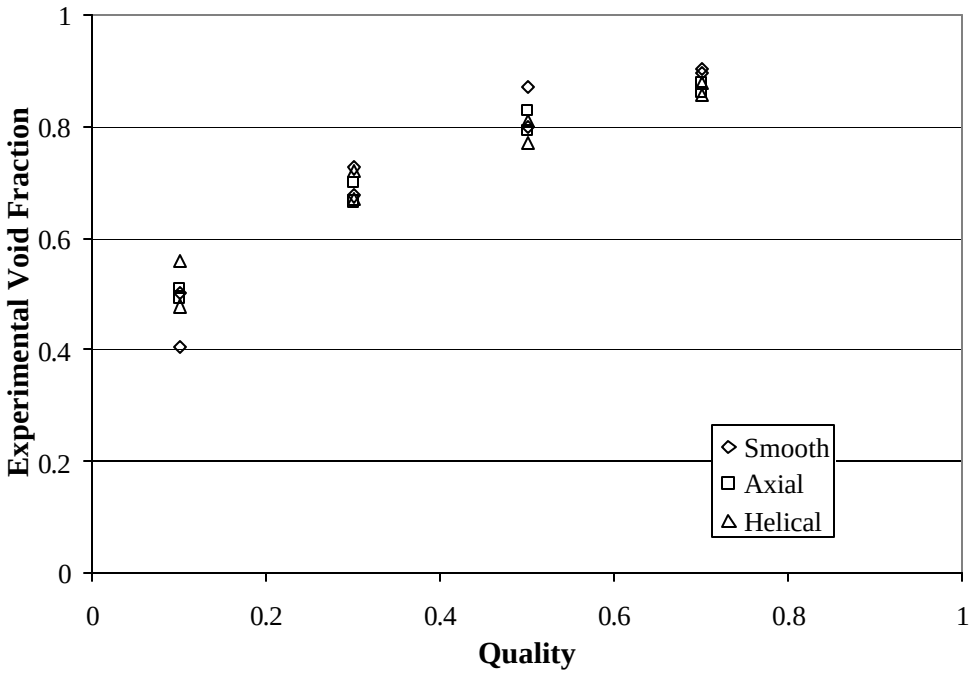

Figure A.1: Experimental Void Fraction vs. Quality for R134a/ 0.2-0.4 % ISO 32 POE, with no rinsing, separated by tube type

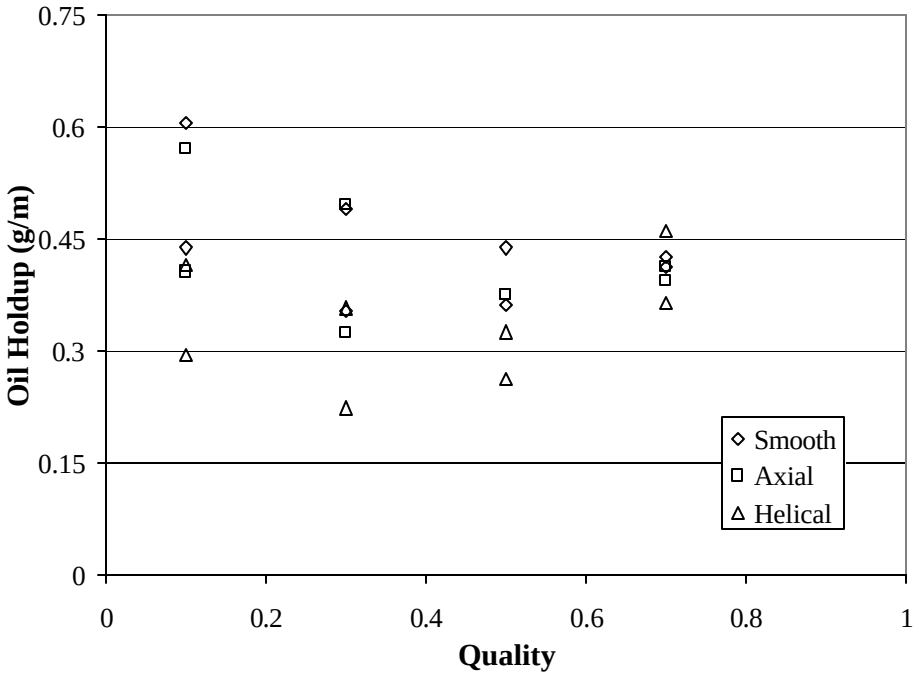

Figure A.2: Oil Holdup (g/m) vs. Quality for R134a/ 0.2-0.4 % ISO 32 POE, with no rinsing, separated by tube type

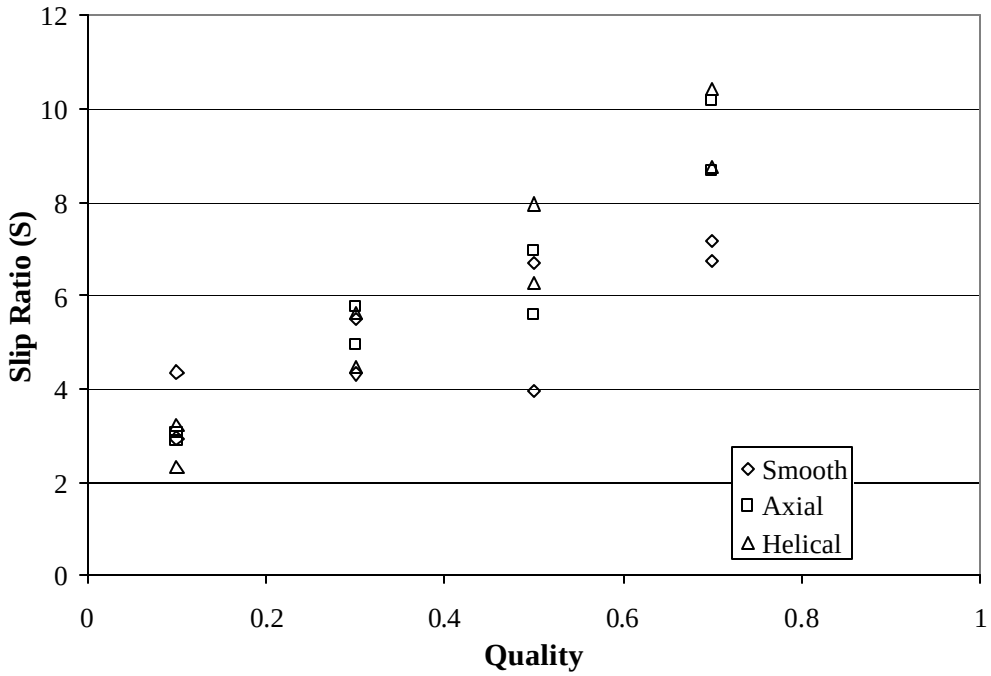

Figure A.3: Slip Ratio vs. Quality for R134a/ 0.2-0.4 % ISO 32 POE, with no rinsing, separated by tube type

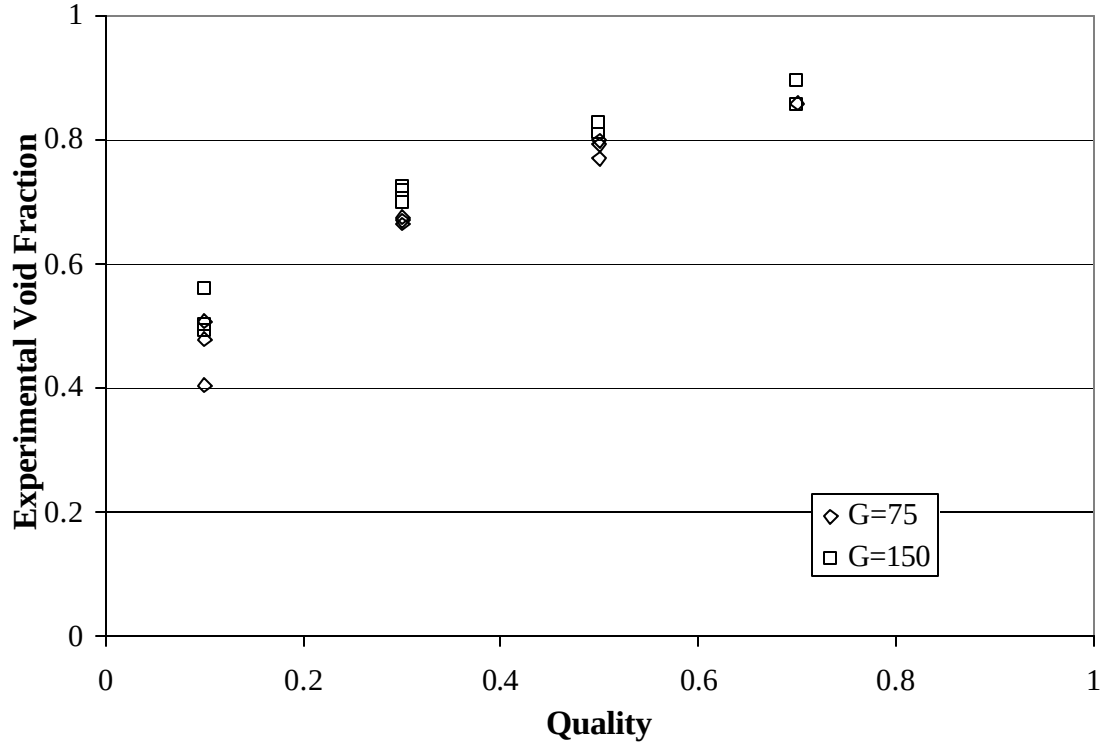

Figure A.4: Experimental Void Fraction vs. Quality for R134a/ 0.2-0.4 % ISO 32 POE, with no rinsing, separated by mass flux

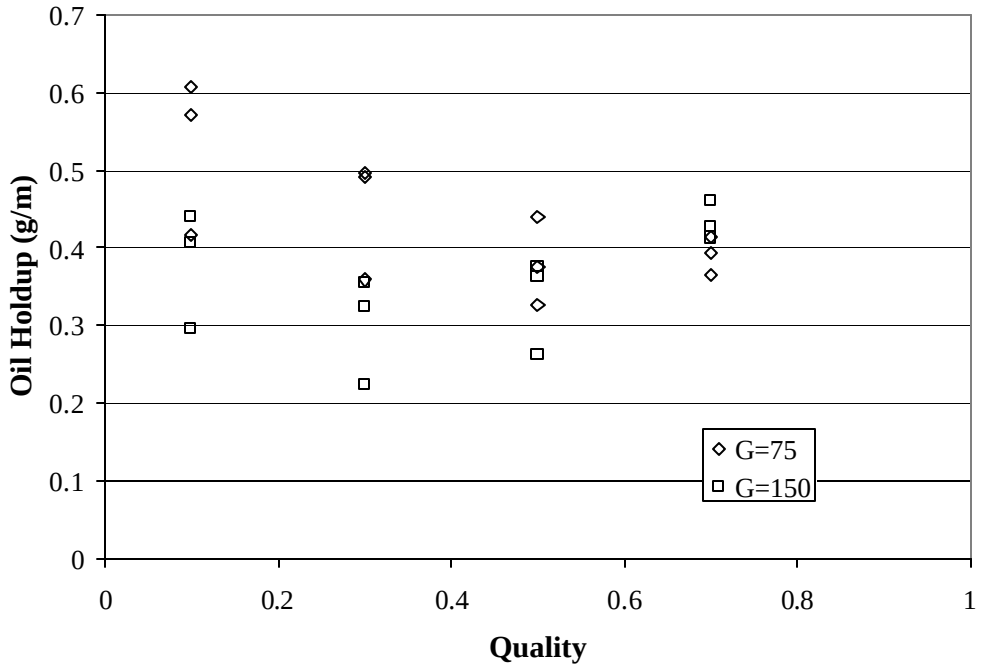

Figure A.5: Oil Holdup (g/m) vs. Quality for R134a/ 0.2-0.4 % ISO 32 POE, with no rinsing, separated by mass flux

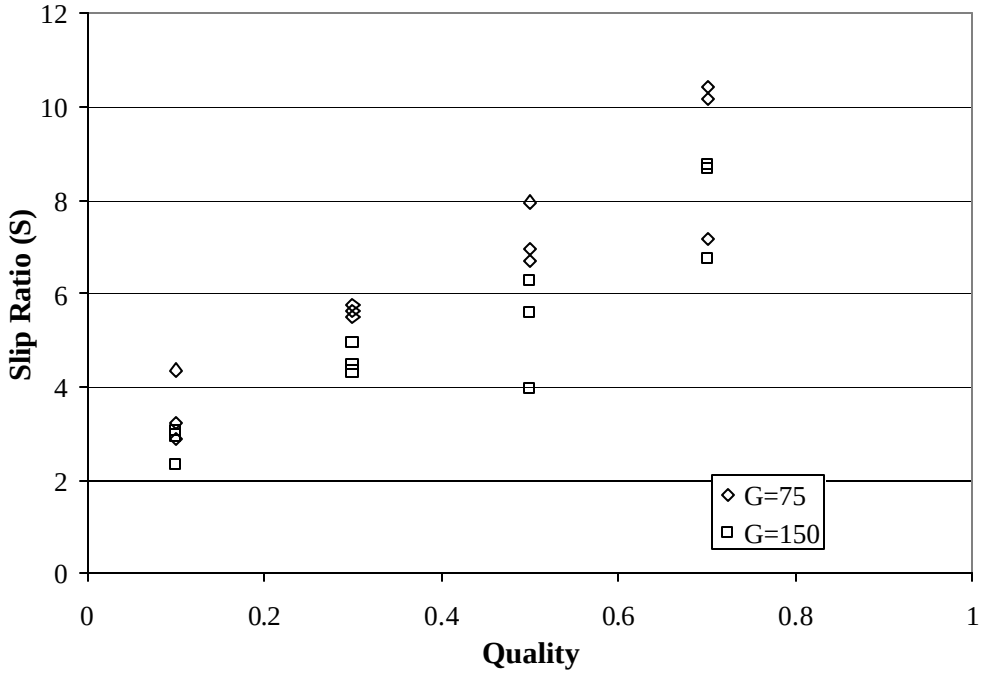

Figure A.6: Slip Ratio vs. Quality for R134a/ 0.2-0.4 % ISO 32 POE, with no rinsing, separated by mass flux

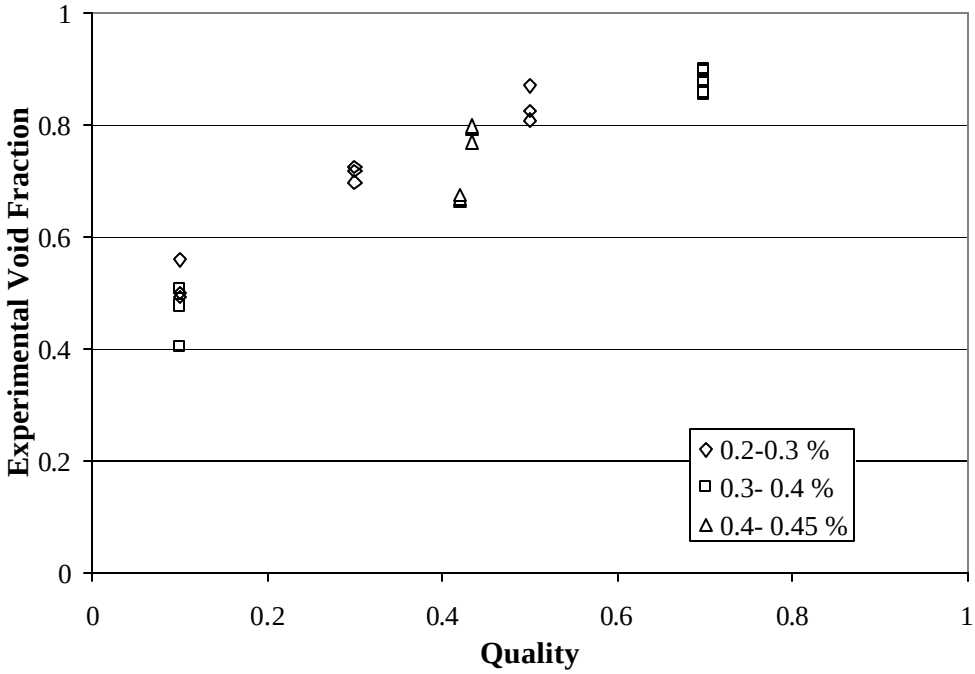

Figure A.7: Experimental Void Fraction vs. Quality for R134a/ 0.2-0.4 % ISO 32 POE, with no rinsing, separated by oil concentration

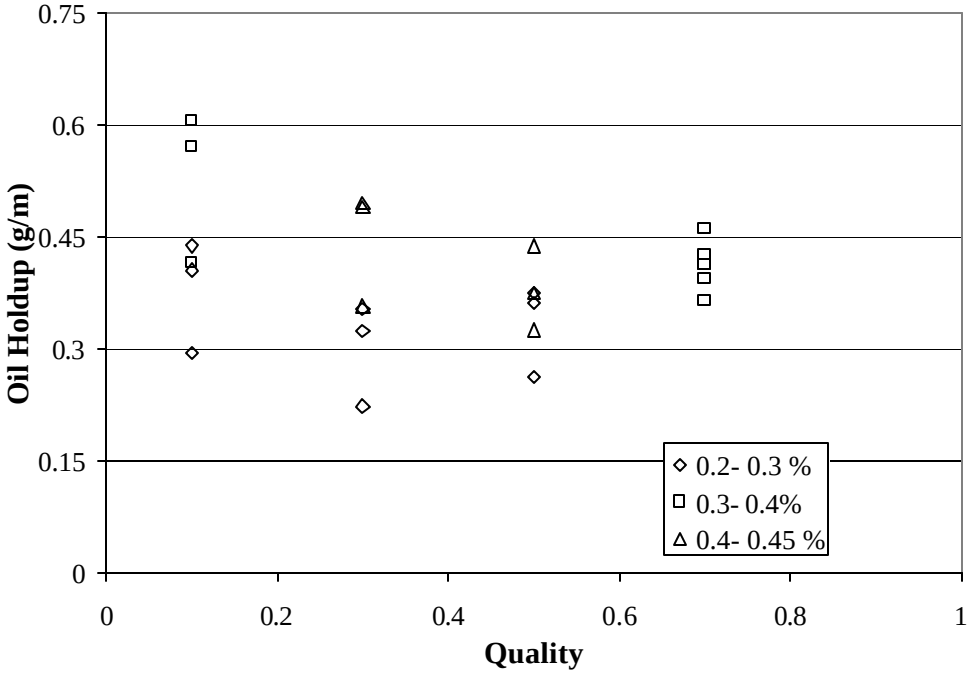

Figure A.8: Oil Holdup (g/m) vs. Quality for R134a/ 0.2-0.4 % ISO 32 POE, with no rinsing, separated by oil concentration

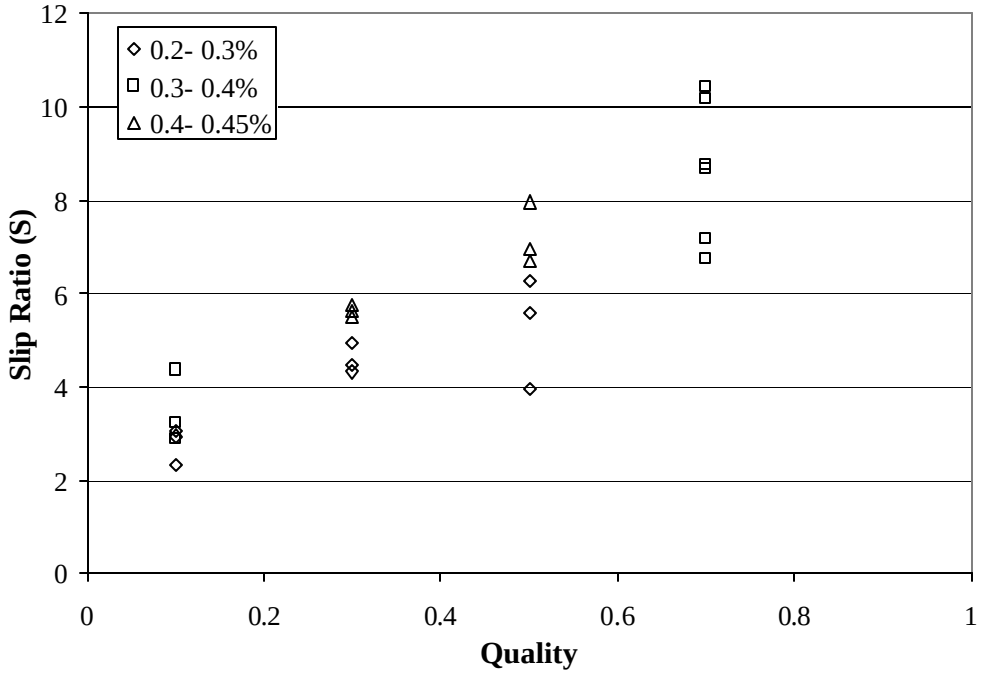

Figure A.9: Slip Ratio vs. Quality for R134a/ 0.2-0.4 % ISO 32 POE, with no rinsing, separated by oil concentration

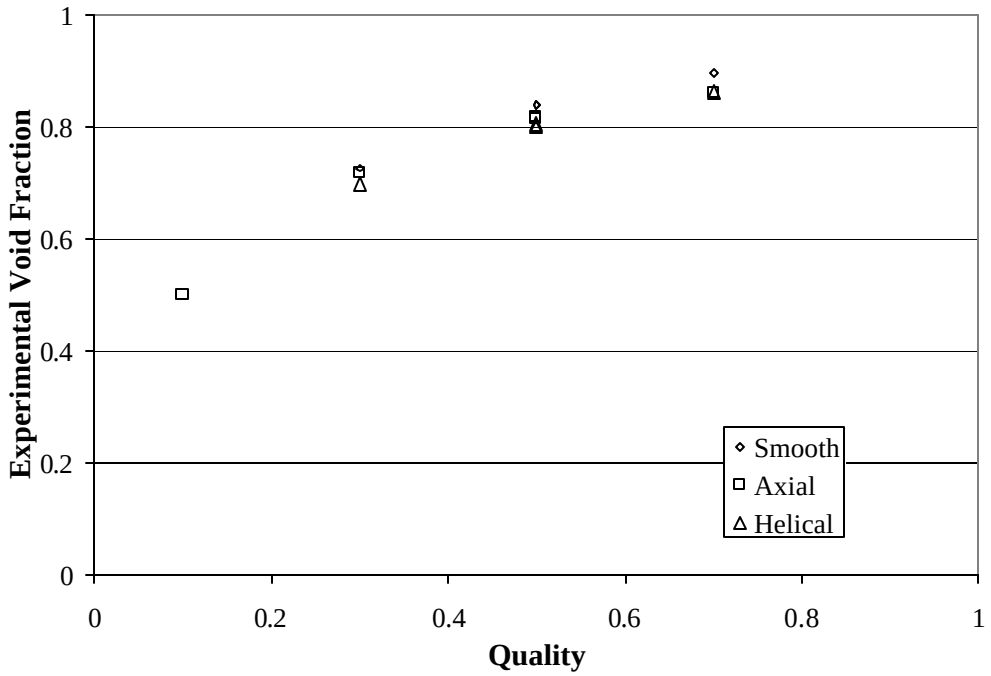

Figure A.10: Void Fraction vs. Quality for R134a/ 6-7 % ISO 32 POE, with no rinsing, G=150, separated by tube type

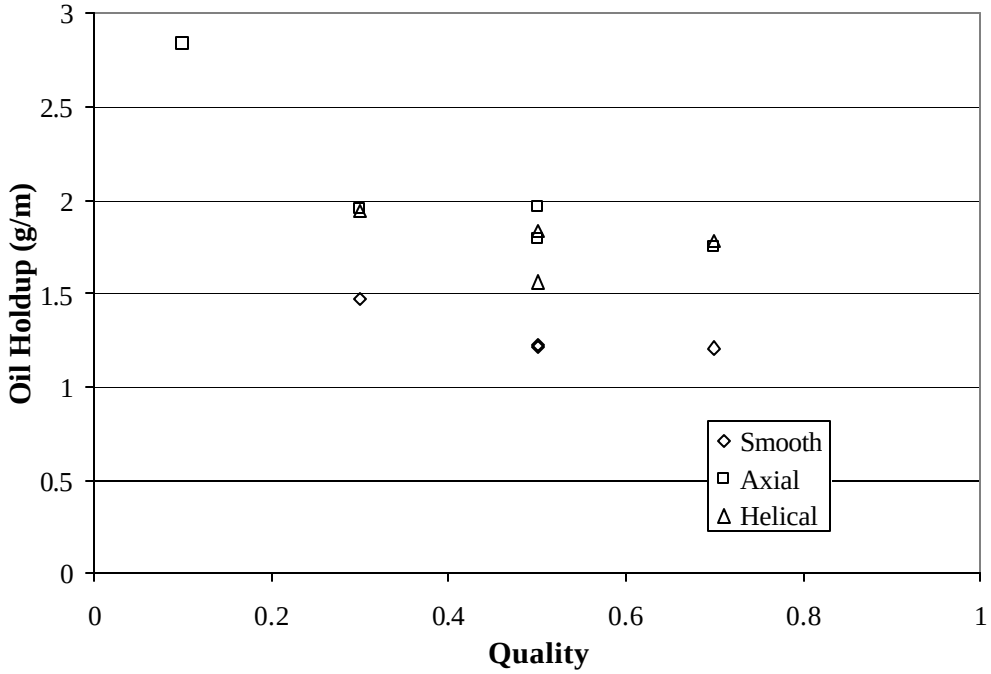

Figure A.11: Oil Holdup vs. Quality for R134a/ 6-7 % ISO 32 POE, with no rinsing, G=150, separated by tube type

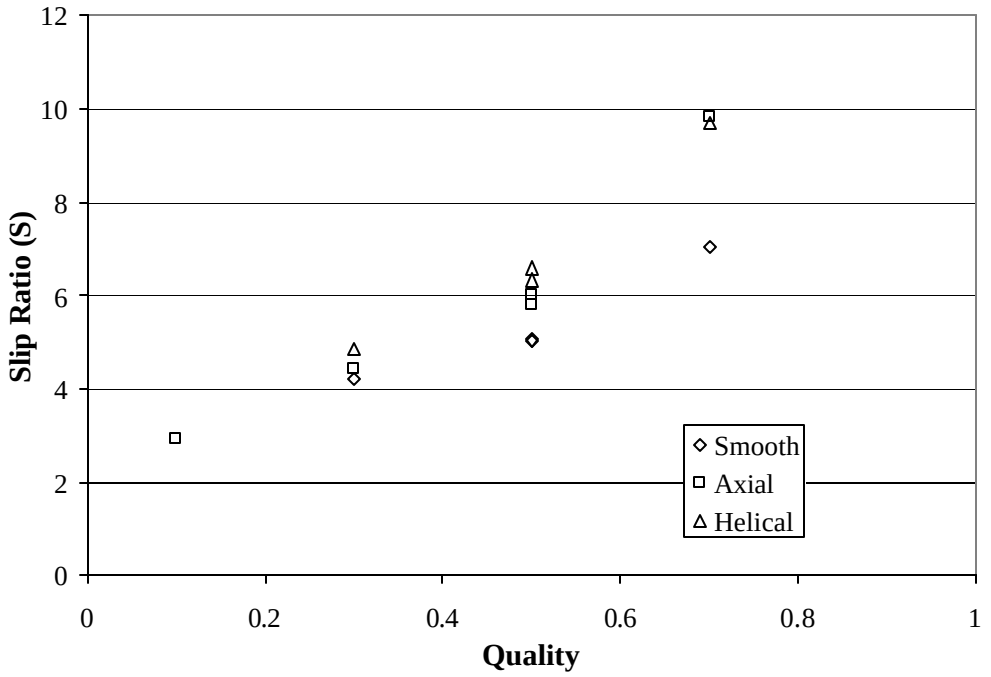

Figure A.12: Slip Ratio vs. Quality for R134a/ 6-7 % ISO 32 POE, with no rinsing, G=150, separated by tube type

Table A.1: Smooth Test Section Experimental Results

G $(\frac{kg}{m^2 s})$	x	Oil Conc. (%)	α	Oil Holdup (g)	Slip Ratio (S)
75	0.1	0.326	0.405	0.94	4.36
75	0.3	0.421	0.676	0.76	5.50
75	0.5	0.434	0.800	0.68	6.70
75	0.7	0.398	0.897	0.64	7.17
150	0.1	0.197	0.502	0.68	2.95
150	0.3	0.281	0.726	0.55	4.32
150	0.3	6.038	0.728	2.62	4.23
150	0.5	0.207	0.871	0.56	3.96
150	0.5	6.23	0.840	2.24	5.05
150	0.5	6.343	0.840	2.67	5.02
150	0.7	0.377	0.903	0.66	6.73
150	0.7	6.258	0.897	2.11	7.05

Table A.2: Axial Test Section Experimental Results

G $(\frac{kg}{m^2 s})$	x	Oil Conc. (%)	α	Oil Holdup (g)	Slip Ratio (S)
75	0.1	0.326	0.508	0.90	2.87
75	0.3	0.421	0.665	0.78	5.76
75	0.5	0.434	0.793	0.59	6.95
75	0.7	0.398	0.860	0.62	10.18
150	0.1	0.197	0.493	0.64	3.06
150	0.1	7.002	0.500	4.47	2.92
150	0.3	0.281	0.699	0.51	4.92
150	0.3	6.038	0.718	3.08	4.44
150	0.5	0.207	0.827	0.59	5.60
150	0.5	6.230	0.820	2.82	5.80
150	0.5	6.343	0.815	3.09	6.01
150	0.7	0.377	0.878	0.65	8.66
150	0.7	6.258	0.862	2.75	9.83

Table A.3: Helical Test Section Experimental Results

G $(\frac{kg}{m^2 s})$	x	Oil Conc. (%)	α	Oil Holdup (g)	Slip Ratio (S)
75	0.1	0.326	0.479	0.65	3.23
75	0.3	0.421	0.671	0.56	5.62
75	0.5	0.434	0.770	0.51	7.96
75	0.7	0.398	0.857	0.57	10.43
150	0.1	0.197	0.560	0.46	2.33
150	0.3	0.281	0.720	0.35	4.46
150	0.3	6.038	0.699	3.03	4.87
150	0.5	0.207	0.810	0.41	6.27
150	0.5	6.23	0.807	2.44	6.33
150	0.5	6.343	0.800	2.87	6.59
150	0.7	0.377	0.877	0.72	8.77
150	0.7	6.258	0.864	2.78	9.70

Appendix B: Experimental Data for Experiments with Rinsing

Table B.1: Smooth Test Section Experimental Results (V_{ts}= 9.65E-5 m^3)

G ($\frac{kg}{m^2 s}$)	x	Oil Conc. (%)	α	Refrigerant Weight (g)	Oil Holdup (g)	Slip Ratio (S)
75	0.1	2.988	0.563	49.74	1.63	2.30
75	0.1	0.188	0.559	52.06	0.03	2.34
75	0.3	3.002	0.749	30.02	1.23	3.82
75	0.5	3.258	0.831	21.36	0.97	5.39
75	0.5	0.114	0.839	21.65	0	5.11
75	0.7	3.523	0.906	13.4	0.84	6.42
75	0.8	3.042	0.935	10.25	0.85	7.38
75	0.9	2.763	0.939	9.69	0.97	15.58
75	0.9	0.188	0.975	6.91	0	6.11
75	0.95	2.763	0.959	7.33	1.08	21.37
75	0.95	0.188	0.971	7.31	0.02	15.00
150	0.1	2.062	0.548	47.89	1.69	2.44
150	0.1	1.136	0.561	51.66	0.14	2.32
150	0.3	2.186	0.760	27.69	0.55	3.60
150	0.5	1.648	0.833	20.29	0.55	5.35
150	0.8	2.789	0.947	9.15	0.7	5.97
150	0.9	3.063	0.953	8.15	0.96	11.75
150	0.9	0.160	0.97	7.05	0	6.44
150	0.95	2.749	0.963	6.69	1.33	19.66
150	0.95	0.160	0.967	7.81	0.03	17.55

Table B.2: Axial Test Section Experimental Results (V_{ts}= 9.605E-5 m^3)

G ($\frac{kg}{m^2 s}$)	x	Oil Conc. (%)	α	Refrigerant Weight (g)	Oil Holdup (g)	Slip Ratio (S)
75	0.1	2.988	0.505	55.61	1.69	2.89
75	0.1	0.188	0.502	57.8	0.15	2.94
75	0.3	3.002	0.713	33.69	1.29	4.59
75	0.5	3.258	0.791	25.35	1.22	7.03
75	0.5	0.114	0.792	26.67	0	7.02
75	0.7	3.523	0.880	15.9	1.07	8.46
75	0.8	3.042	0.924	11.57	0.74	8.80
75	0.9	2.763	0.939	9.46	1.09	15.49
75	0.9	0.188	0.942	10.47	0.03	14.91
75	0.95	2.763	0.937	9.41	1.31	33.83
75	0.95	0.188	0.972	7.27	0	14.85
150	0.1	2.062	0.512	55.15	1.66	2.82
150	0.1	0.112	0.486	59.62	0.06	3.14
150	0.3	2.186	0.716	34.02	0.8	4.52
150	0.5	1.648	0.829	22.2	0.48	5.50
150	0.8	2.789	0.916	11.96	1.1	9.76
150	0.9	3.063	0.927	9.99	1.71	18.72
150	0.9	0.160	0.941	10.63	0	15.22
150	0.95	2.749	0.943	8.21	1.8	30.60
150	0.95	0.160	0.958	8.77	0	22.43

Table B.3: Helical Test Section Experimental Results (V_{ts}= 9.695E-5 m^3)

G ($\frac{kg}{m^2 s}$)	x	Oil Conc. (%)	α	Refrigerant Weight (g)	Oil Holdup (g)	Slip Ratio (S)
75	0.1	2.988	0.506	55.94	1.84	2.89
75	0.1	0.188	0.539	54.4	0.06	2.54
75	0.3	3.002	0.736	31.41	1.34	4.08
75	0.5	3.258	0.782	26.4	1.33	7.40
75	0.5	0.114	0.792	26.96	0	7.03
75	0.7	3.523	0.880	16.16	1.01	8.48
75	0.8	3.042	0.901	13.48	1.28	11.65
75	0.9	2.763	0.919	11.23	1.52	21.04
75	0.9	0.188	0.924	12.46	0.03	19.7
75	0.95	2.763	0.920	10.19	2.28	43.72
75	0.95	0.188	0.922	12.6	0.12	42.94
150	0.1	2.062	0.520	53.19	1.84	2.73
150	0.1	0.112	0.514	57.18	0.08	2.81
150	0.3	2.186	0.709	34.21	0.86	4.69
150	0.5	1.648	0.828	21.75	0.66	5.54
150	0.8	2.789	0.914	12.44	0.97	9.99
150	0.9	3.063	0.927	10.34	1.53	18.77
150	0.9	0.160	0.949	9.69	0.05	12.8
150	0.95	2.749	0.938	8.82	1.82	33.41
150	0.95	0.160	0.943	10.33	0.09	30.60

Appendix C: Modeling Results for Oil Mixtures

Table C.1: Predicted Void Fractions with ACRC Void Fraction Model for Smooth Test Section

a (exper.)	x	G	a (pure ref. properties)	a (Baustian Model)	a (Cawte Model)	a (Linear Model)
0.5625	0.1	75	0.5062	0.5047	0.5056	0.4996
0.5588	0.1	75	0.5062	0.5061	0.5062	0.5053
0.7486	0.3	75	0.747	0.7442	0.7458	0.7359
0.8313	0.5	75	0.8561	0.8529	0.8548	0.8452
0.8394	0.5	75	0.8561	0.856	0.8561	0.8549
0.9061	0.7	75	0.9213	0.918	0.9199	0.9126
0.935	0.8	75	0.9462	0.9435	0.945	0.9397
0.9389	0.9	75	0.969	0.9668	0.9679	0.9648
0.9752	0.9	75	0.969	0.9687	0.9689	0.9676
0.9594	0.95	75	0.9808	0.9791	0.9799	0.9782
0.9713	0.95	75	0.9808	0.9806	0.9807	0.9797
0.5478	0.1	150	0.5753	0.5735	0.5745	0.5661
0.5613	0.1	150	0.5753	0.5743	0.5749	0.5688
0.76	0.3	150	0.7984	0.7957	0.7973	0.786
0.8328	0.5	150	0.8896	0.8875	0.8887	0.8802
0.9468	0.8	150	0.9613	0.9585	0.9601	0.9545
0.9532	0.9	150	0.9787	0.9763	0.9775	0.9743
0.9739	0.9	150	0.9787	0.9785	0.9786	0.9774
0.9625	0.95	150	0.9874	0.9857	0.9865	0.9847
0.9666	0.95	150	0.9874	0.9872	0.9873	0.9864

Table C.2: Predicted Void Fractions with ACRC Void Fraction Model for Axial Test Section

a (exper.)	x	G	a (pure ref. properties)	a (Baustian Model)	a (Cawte Model)	a (Linear Model)
0.5052	0.1	75	0.4515	0.4499	0.4508	0.4445
0.5021	0.1	75	0.4515	0.4514	0.4514	0.4505
0.7126	0.3	75	0.7112	0.7081	0.7099	0.6989
0.7906	0.5	75	0.834	0.8304	0.8325	0.8216
0.792	0.5	75	0.834	0.8339	0.834	0.8326
0.8798	0.7	75	0.9087	0.9049	0.9071	0.8987
0.9235	0.8	75	0.9374	0.9343	0.9361	0.9299
0.9392	0.9	75	0.9638	0.9613	0.9626	0.959
0.9416	0.9	75	0.9638	0.9636	0.9637	0.9622
0.9372	0.95	75	0.9776	0.9756	0.9765	0.9746
0.9716	0.95	75	0.9776	0.9773	0.9775	0.9764
0.5117	0.1	150	0.5242	0.5223	0.5234	0.5144
0.4862	0.1	150	0.5242	0.5241	0.5241	0.5231
0.7162	0.3	150	0.7687	0.7657	0.7675	0.7548
0.8288	0.5	150	0.8722	0.8699	0.8713	0.8615
0.9159	0.8	150	0.9549	0.9517	0.9535	0.9471
0.9274	0.9	150	0.9751	0.9723	0.9738	0.97
0.9405	0.9	150	0.9751	0.9749	0.9751	0.9736
0.9429	0.95	150	0.9853	0.9833	0.9842	0.9822
0.9577	0.95	150	0.9853	0.9851	0.9852	0.9841

Table C.3: Predicted Void Fractions with ACRC Void Fraction Model for Helical Test Section

a (exper.)	x	G	a (pure ref. properties)	a (Baustian Model)	a (Cawte Model)	a (Linear Model)
0.5055	0.1	75	0.4515	0.4499	0.4508	0.4445
0.5392	0.1	75	0.4515	0.4514	0.4514	0.4505
0.736	0.3	75	0.7112	0.7081	0.7099	0.6989
0.7821	0.5	75	0.834	0.8304	0.8325	0.8216
0.7916	0.5	75	0.834	0.8339	0.834	0.8326
0.8795	0.7	75	0.9087	0.9049	0.9071	0.8987
0.9011	0.8	75	0.9374	0.9343	0.9361	0.9299
0.9191	0.9	75	0.9638	0.9613	0.9626	0.959
0.9243	0.9	75	0.9638	0.9636	0.9637	0.9622
0.9203	0.95	75	0.9776	0.9756	0.9765	0.9746
0.922	0.95	75	0.9776	0.9773	0.9775	0.9764
0.5199	0.1	150	0.5242	0.5223	0.5234	0.5144
0.5135	0.1	150	0.5242	0.5241	0.5241	0.5231
0.7087	0.3	150	0.7687	0.7657	0.7675	0.7548
0.8277	0.5	150	0.8722	0.8699	0.8713	0.8615
0.9141	0.8	150	0.9549	0.9517	0.9535	0.9471
0.9272	0.9	150	0.9751	0.9723	0.9738	0.97
0.9494	0.9	150	0.9751	0.9749	0.9751	0.9736
0.9379	0.95	150	0.9853	0.9833	0.9842	0.9822
0.9431	0.95	150	0.9853	0.9851	0.9852	0.9841